

# Option-Implied Bounds for the Crash Probability of a Stock

Ran Shi <sup>\*</sup>

October 2021

## Abstract

I propose a framework to compute sharp bounds of the crash probability of an individual stock using option prices. Empirical tests suggest that these bounds are close to the exact forward-looking crash probabilities. They drive out stock characteristics reported in the literature in terms of explaining crash probability variation. Out of sample, either the lower or upper bound outperforms combinations of stock characteristics in terms of forecasting stock-specific crash events. Applying the framework to study the equity of global systemically important banks (G-SIBs) gives rise to forward-looking fragility and stability measures of the global financial system.

---

<sup>\*</sup>[r.shi1@lse.ac.uk](mailto:r.shi1@lse.ac.uk), Department of Finance, London School of Economics. I thank Bertram Düring, Christopher Jones, Christian Julliard, Lukas Kremens, Igor Makarov, Ian Martin, and Shixiang Xia for their comments.

*“It is better to be vaguely right than exactly wrong.”*

— Carveth Read, *Logic, Deductive and Inductive*

Using option prices, I develop a theoretical framework to bound the expectation of a payoff that is contingent on a stock return. Both the lower and upper bounds are available from this framework and they are sharp in theory. I apply this framework to calculate forecasting bounds for stock crash probabilities. The crash probability bounds appear to be tight throughout empirical tests<sup>1</sup>. I show further that these bounds can forecast crash events out-of-sample, and they outperform combinations of various stock characteristics documented in the existing literature that are related to crash risk.<sup>2</sup>

The bounds are constructed from (and only from) current security prices, thus no historical data are needed. This feature enables real-time forecasting, which can offer timely insights into the downside risk of an individual stock. In theory, they can bound the probability of a single-stock crash event any time in the future (of course, in reality, their forecasting horizons are limited by maturities of option contracts). Their timeliness is only constrained by “freshness” of security prices.

Compared with interval forecasts generated from statistical procedures, these option-implied bounds are probabilistic with guaranteed coverage in theory. In other words, these forecasting bounds have 100% “confidence levels” in the sense of traditional statistical inference. As Keynes has noted in his 1921 book *A Treatise on Probability*: “Many probabilities, which are incapable of numerical measurement, can be placed nevertheless between numerical limits.” It is exactly the same notion that motivates these forecasting bounds with guaranteed coverage.

These forecasting bounds are robust in that they do not impose any distributional assumptions on the stock returns at any time. Their sharpness remains when stock returns contain components like stochastic volatility and jump. This important feature is a strength of my methodology, since stock returns exhibit complicated time-varying distributional patterns ([Andersen, Bollerslev, Diebold, and Ebens, 2001](#); [Andersen, Benzoni, and Lund, 2002](#)).

The bounds are derived by applying the probability theory of copula functions. The methodological framework is streamlined into two steps: recovering risk-neutral (marginal) distributions

---

<sup>1</sup>To clarify, sharpness refers to the result that the bounds cannot be further improved without leveraging additional data (for example, high-equality basket option prices in deep markets, which are not available in practice) or making additional assumptions (which can be fragile). Tightness describes the fact that both the lower and upper bounds are close to the true crash probability. The former is a theoretical property and the latter is an empirical phenomenon.

<sup>2</sup>See, for example, [Chen, Hong, and Stein \(2001\)](#); [Boyer, Mitton, and Vorkink \(2009\)](#) and [Greenwood, Shleifer, and You \(2018\)](#).

of stock and market returns from option prices first (applying the well-known approach of [Breen and Litzenberger \(1978\)](#)), then bounding the physical (in contrast to the risk-neutral) expectations using copula theory (the Fréchet-Hoeffding bounds). In short, the method can be branded as “Breen-Litzenberger meets Fréchet-Hoeffding”.

The underlying theory guarantees sharpness of these bounds. In order to achieve meaningful performance improvement, one needs solid knowledge regarding risk-neutral correlations between single-stock and market returns, that is, the market price of correlation risk. Practically, it is difficult to observe or back out these prices that are not mired by microstructural issues, without having deep markets of basket options on both single-stock prices and the market index. Theoretically, it is also dangerous to impose *ad-hoc* assumptions on the correlation risk (and its price): the 2008 financial crisis offers hard lessons on the mispricing of correlation risk.

I now turn to the empirics. I compute the crash probability bounds for stocks belonging to the S&P 500 index. These bounds target on the probabilities of 5%, 10% and 20% crashes in one month, one quarter, six months and one year. They demonstrate significant variations across firms. For example, the time-series averaged probabilities of a 20% crash in one year can be as low as within [4.6%, 13.0%] for some firm, and as high as within [34.0%, 55.7%] for another firm.

These forecasting bounds also vary significantly across time. In [Figure 1](#), I plot the monthly forecasting bounds for the probability of a crash that is worse than 20% over the one-year horizon for two companies: Cisco and AIG. Cisco had the largest market capitalization on March, 2000 during the dot-com bubble. According to [Figure 1](#), its crash probabilities started climbing up during the second half of 2000 and peaked in early 2001, being over 35% to 50%. In reality, its market capitalization had dropped more than 70% by the end of 2001. The other company in [Figure 1](#) is AIG, which was in the eye of the tornado during the subprime crisis. Its crash probability started surging rapidly from the late 2007, almost one year ahead of the paramount outbreak of the crisis in October, 2008. The crash probability peaked at over 55% to 80% during the crisis.

I test the tightness of these bounds by regressing the future crash event indicators directly on the crash probability bounds<sup>3</sup>. If the bounds are tight, they should both be very close to the true crash probability. Since the crash probability is the expectation of the crash event indicator, tight bounds will deliver intercepts of zero and slopes of one consistently throughout the regressions. These hypotheses are strongly supported by the data. Across different regression settings, the

---

<sup>3</sup>A crash event is defined as the stock return being smaller than a certain threshold, say, the gross return of a stock being smaller than 0.80 is a 20% crash event. A crash event indicator is a binary variable that equals one if the crash does happen and zero otherwise.

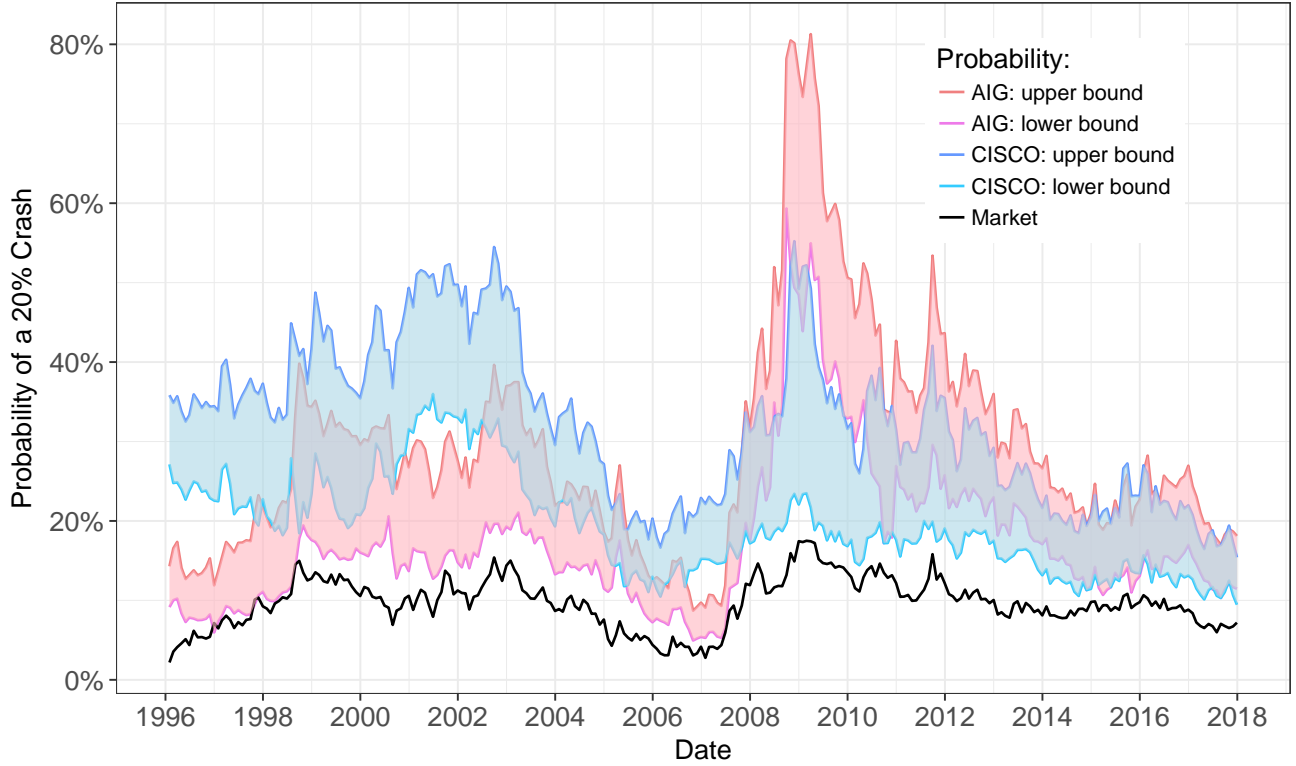


Figure 1: Monthly forward-looking probabilities of a crash (one-year net returns being less than  $-20\%$ ): Cisco stock, AIG stock, and the market (S&P 500). The forecasting bounds for stocks are based on the approach presented in this paper. The point forecast for the crash probability of the market is based on the approach in [Martin \(2017\)](#).

intercepts are mostly not significantly different from zero. On the contrary, the slopes are highly significant and, more importantly, they are extremely close to one, especially for the lower bound.

I then include stock characteristics, which have been reported in the previous literature to be related to crashes, into the regressions. The regression slopes for my bounds are still significantly different from zero, suggesting that they continue explaining variation in the crash probability. The slopes for the lower bound are still very close to one. The adjusted- $R^2$ s in most of these regressions drop after including these characteristics. These evidence further suggest that the theory-motivated bounds drive out stock characteristics in terms of explaining variation in the crash probability.

Out-of-sample predictive performance of the bounds is evaluated against the combination of over ten stock characteristics. I design a procedure to emulate an avid “data-snooper” in order to compete against my single forecasting variable (either the lower or the upper bound). In doing so, I split the dataset into a training and a testing sample. The stock characteristics are combined through linear regressions, as well as logistic regressions, by fitting them to the training

sample. In addition, when fitting these models, I add-in a “machine learning” flavor by using  $\ell_1$  penalty (as known as the LASSO in the statistics literature, see, for example, [Tibshirani \(1996\)](#)) to select “best” possible models through cross-validation (in the training sample). The predictive power of forecasting bounds is then compared with this pure data-mining procedure. The theory motivated bounds consistently outperform predictors extracted from stock characteristics across all forecasting horizons.

These crash probability bounds is then applied to study the declines in the equity of global systemically important banks (G-SIBs). I first compute the crash probability bounds for the majority of G-SIBs across different time. Then I aggregate these bounds across banks based on simple probability inequalities to created fragility and stability measures of the global banking system. These two measures help illustrate the many potential applications of these bounds in terms of creating macroeconomic indicators.

*Related Literature.* Asset pricing bounds have been derived for contingent claims in the context of incomplete markets or market imperfections ([Cochrane and Saá-Requejo, 2000](#); [Bernardo and Ledoit, 2000](#); [Constantinides et al., 2008](#)). Instead of bounding contingent claim prices that are determined by risk-neutral expectations, this paper establishes a new robust framework to compute bounds for physical expectations of contingent claims.

A large literature proposes methods to recover risk-neutral probabilities from option prices. An incomplete list includes [Breedon and Litzenberger \(1978\)](#); [Jackwerth and Rubinstein \(1996\)](#); [Aït-Sahalia and Lo \(1998\)](#); [Rubinstein \(1994\)](#). While the starting point of my derivation relies on the insights of [Breedon and Litzenberger \(1978\)](#), the major challenge of bounding the physical expectations are addressed by the new approaches introduced in this paper.

A few papers have attempted to forecast crashes in the stock market. [Chen, Hong, and Stein \(2001\)](#) use characteristics such as (detrended) trading volume and past returns to forecast negative skewness in the cross-section of individual stocks. [Greenwood et al. \(2018\)](#) use characteristics to forecast crashes at the industry level conditional on observing past price surge. [Bates \(1991\)](#) finds evidences from put option prices that forecast the stock market crash of 1987 (Black Monday). There is also a (downside/skewness/tail) risk literature that measures related objects as this paper does, but their main focus are how these risks manifest themselves into the cross-section of expected stock returns (see, for example, [Ang, Chen, and Xing \(2006\)](#); [Boyer, Mitton, and Vorkink \(2009\)](#); [Kelly and Jiang \(2014\)](#)). [Martin \(2017\)](#) has a section on recovering the physical crash probability of the market (which I have adapted to include in Figure 1), but going from the market crash to individual stock crash is not straightforward.

The rest of this paper is organized as follows. Section 1 introduces the underlying theory and method, as well as discusses theoretical properties of the bounds. Section 2 provides details of my data sample. Section 3 presents my empirical results. Section 4 includes extensions of the framework in terms of generalization and application. Section 5 concludes. All proofs for theoretical results are available in the Appendix unless otherwise noted.

# 1 Theory and Method

## 1.1 A simple link between the physical expectation and the risk-neutral expectation

To begin with, consider an investor who chooses to invest fully into the market of risky assets. The investor derives utility from her terminal wealth with a power utility function  $u(x) = u^{1-\gamma}/(1-\gamma)$ . The investor's portfolio choice problem is then<sup>4</sup>

$$\underset{w}{\text{maximize}} \quad \mathbb{E} \left[ u \left( w^\top R \right) \right], \quad \text{subject to} \quad \sum_i^n w_i = 1,$$

where the random vector  $R = [R_1, \dots, R_n]^\top$  concatenates gross returns on all risky assets; the choice variables in  $w = [w_1, \dots, w_n]^\top$  capture the investor's portfolio weights. The first-order conditions for this problem are

$$\mathbb{E} \left[ \left( w^{\star\top} R \right)^{-\gamma} R_i \right] = \lambda \quad \text{for all } i,$$

where  $\lambda$  is a Lagrangian multiplier; the superscript  $\star$  represents solutions to the optimization problem. By assumption, this investor chooses to invest fully in the market, thus the market return, denoted by  $R_m$ , is such that  $R_m = w^{\star\top} R$ . Plugging  $R_m$  into the first-order conditions, a direct implication is that  $R_m^{-\gamma}/\lambda$  is a stochastic discount factor (SDF) because

$$\mathbb{E}[MR_i] = 1 \quad \text{for all } i,$$

where

$$M = R_m^{-\gamma}/\lambda$$

is the SDF due to this specific marginal investor.

Assuming that there is no arbitrage, for any random payoff of interest  $X$ , the *risk-neutral*

---

<sup>4</sup>For clarity and the ease of exposition, I suppress the unnecessary time subscript because the following theory and method are static in nature. However, it is worthwhile noting the whole framework is constructed on one-period ahead conditional probabilities.

expectation of  $X$  must satisfy the following equation

$$\frac{1}{R_f} \mathbb{E}^*[X] = \mathbb{E}[MX],$$

where  $R_f$  is the risk-free rate. The equation holds because both sides calculate today's price of a claim to the random payoff  $X$ <sup>5</sup>. This equation, combined with the SDF induced by the investor's marginal behavior, can be used to determine physical expectations for the random payoff of interest<sup>6</sup>. To be specific,

$$\mathbb{E}[X] = \mathbb{E}[\underbrace{M \lambda R_m^\gamma}_{\equiv 1} X] = \lambda \mathbb{E}[M(R_m^\gamma X)] = \frac{\lambda}{R_f} \mathbb{E}^*[R_m^\gamma X].$$

Plugging in a special constant payoff  $X = 1$  to the equation above,

$$1 = \frac{\lambda}{R_f} \mathbb{E}^*[R_m^\gamma].$$

Dividing the two equations we just have,

$$\mathbb{E}[X] = \frac{\mathbb{E}^*[R_m^\gamma X]}{\mathbb{E}^*[R_m^\gamma]}. \quad (1)$$

There are many potential applications of equation (1) in terms of characterizing the behaviors of individual stock returns. For example, for a given constant  $q$ , if we let  $X = I(R_i \leq q)$ , where  $I(\cdot)$  equals one if the event in the parentheses is true and zero if not, equation (1) implies that

$$\mathbb{P}[R_i \leq q] = \frac{\mathbb{E}^*[R_m^\gamma I(R_i \leq q)]}{\mathbb{E}^*[R_m^\gamma]}, \quad (2)$$

because  $\mathbb{P}[R_i \leq q] = \mathbb{E}[I(R_i \leq q)]$ . Equation (2) shows that one can fully recover the physical probability distribution of a particular stock return, as perceived by the power-utility investor who is holding the market, from risk-neutral distributions. Physical distributions computed this way are forward-looking, which make them useful for real-time forecasting. A direct application is forecasting the crash probability of a stock, as I will demonstrate throughout the rest of this paper.

Another case is that one can simply let  $X$  be the return on a stock, that is,  $X = R_i$  for some  $i$ , the expected return of this stock,  $\mathbb{E}[R_i]$ , can be given as

$$\mathbb{E}[R_i] = \frac{\mathbb{E}^*[R_m^\gamma R_i]}{\mathbb{E}^*[R_m^\gamma]}. \quad (3)$$

---

<sup>5</sup>Here an implicit assumption is that the power-utility investor is marginal across all markets, including the option markets. In the mean time, she still chooses to hold the market portfolio according to our initial assumption.

<sup>6</sup>Strictly speaking, the expectation operator here is taken under the investor's subjective probabilities instead of the "objective" probabilities of an oracle.

A special case of equation (3) is when the relative risk aversion parameter  $\gamma$  equals one. Since  $\mathbb{E}^*[R_m] = R_f$ , equation (3) becomes

$$\mathbb{E}[R_i] = \frac{1}{R_f} \mathbb{E}^*[R_m R_i], \quad (4)$$

where the market portfolio,  $R_m$ , by assumption, is equivalent to the optimal portfolio return for the log investor (because the investor *chooses* to invest fully in the market). This return is also called the growth-optimal (portfolio) return (Latane, 1959; Breiman, 1960). Martin and Wagner (2018), based on this special specification, derive an equation for the expected return of a stock in terms of the risk-neutral variances.

The assumptions and results of this section will hold throughout the rest of this paper.

## 1.2 A framework to derive sharp bounds for physical expectations from option prices

Now we start considering a very general specification for the payoff  $X$ . Let  $X = h(R_i)$ , where  $h : \mathbb{R}_+ \mapsto \mathbb{R}$  is an arbitrary continuous function<sup>7</sup>. That is, we would like to investigate the physical expectation of any well-behaved payoffs contingent on the return of a stock. This setting also helps motivate a methodological framework which might be of interest by itself.

Denote by  $Q_{mi}$  the *joint* cumulative distribution function (CDF) of  $(R_m, R_i)$  under the risk-neutral probability, and by  $Q_m, Q_i$  the *marginal* CDFs of  $R_m, R_i$ , also under the risk-neutral probability. Thus, equation (1) can be rewritten explicitly as

$$\mathbb{E}[h(R_i)] = \frac{\int x^\gamma h(y) dQ_{mi}(x, y)}{\int x^\gamma dQ_m(x)}. \quad (5)$$

Equation (5) simply tells us that if we can fully characterize the risk-neutral joint distribution  $Q_{mi}$ <sup>8</sup>, we can evaluate the expectation of any well-behaved payoff contingent on the return  $R_i$ . As illustrated through equation (2) and (3), we can then calculate the forward-looking probability of a crash (let  $h(R_i) = I(R_i \leq q)$ ) or the expected return (let  $h(R_i) = R_i$ ) of a stock.

Option prices carry rich information about the risk-neutral distributions. The static replication approach in Breeden and Litzenberger (1978) can recover the risk-neutral distributions from prices of options with various strike prices. For example, we can use the prices of index options to recover the risk-neutral (marginal) distribution  $Q_m$  (which can be used to pin down the denominator of the right-hand side of equation (5)), and we can use the prices of equity options for stock  $i$  to recover the risk-neutral (marginal) distribution  $Q_i$ . I provide details about my implementation

<sup>7</sup>Strictly speaking,  $h$  is continuous almost everywhere.

<sup>8</sup>As a by-product, the risk-neutral marginal  $Q_m(x) = \lim_{y \rightarrow \infty} Q_{mi}(x, y)$  will be known to us



of the Breeden and Litzenberger approach in section 1.3.

It is, however, almost impossible to fully characterize the risk-neutral *joint* distribution  $Q_{mi}$ . Widely traded index and equity options with liquid market places are almost exclusively written on one underlying asset. To recover the risk-neutral joint distribution, one needs to observe the prices of many options written on *both* the stock index and the stock of interest<sup>9</sup>. In addition, these options have to vary not only in terms of strike prices, but also in terms of their contingent payoff formats<sup>10</sup>. Needless to say, all these options have to be smoothly traded with high volume and deep market to avoid microstructural issues. In reality, these options are rare (if not nonexistent) and thinly traded, making it infeasible to back out the whole risk-neutral joint distribution of the market return and the stock return. This poses difficulties to the exact evaluation of  $\mathbb{E}[h(R_i)]$  using equation (5).

Although no exact answer can be given to  $\mathbb{E}[h(R_i)]$  under the current framework, sharp bounds can be obtained for it. Bounding this expectation term relies on dissecting the joint distribution into two parts: the marginals and the dependence structure. The marginals can both be regarded as known, as a result of applying the Breeden-Litzenberger approach to option prices. Then minimizing/maximizing across all possible dependence structures can bound the integral in the numerator of (5). To proceed and formalize these arguments, I will introduce some basic probability theories on *copula functions* first<sup>11</sup>.

**Definition 1.** (A two-dimensional copula, or briefly, a copula) A two-dimensional copula is a function  $C : [0, 1]^2 \mapsto [0, 1]$  with the following properties:

1. *C is grounded:*  $C(x, 0) = C(0, y) = 0$  for any  $(x, y)$  in its domain;
2.  $C(x, 1) = x$  and  $C(1, y) = y$  for any  $(x, y)$  in its domain;
3. *C is two-increasing:* for all rectangles  $B = [x_1, y_1] \times [x_2, y_2] \subset [0, 1]^2$ , the *H-volume* of  $B$ , which is defined by

$$V_H(B) = C(x_2, y_2) - C(x_2, y_1) - C(x_1, y_2) + C(x_1, y_1)$$

is non-negative, that is,  $V_H(B) \geq 0$ .

Copula functions play a central role in the distribution theory of multivariate random variables. They are the joint CDFs of two random variables whose marginals are both uniform within

---

<sup>9</sup>Ross (1976) illustrates the use of numerous options to recover the risk-neutral joint densities; Martin (2018) refines Ross's argument and points out the limitations in practice.

<sup>10</sup>Martin (2018) illustrates the use of butterfly option strategies contingent on  $(R_m + \alpha R_i)$  with finely varying  $\alpha$  to recover the joint risk-neutral distribution in theory.

<sup>11</sup>See Nelsen (2007) for a theoretical monologue on this topic.

$[0, 1]$ . In general, for any two random variables, treating their marginals as given, their joint distribution is uniquely determined by a copula function. This conclusion is due to a theorem by [Sklar \(1959\)](#).

**Theorem 1.** (*Sklar, 1959*) Let  $Q$  be the joint CDF for the random vector  $(X, Y)$  with marginal CDFs  $F_X$  and  $F_Y$ . Then there exists a copula  $C$ , such that for all  $x, y \in \mathbb{R}$ ,

$$Q(x, y) = C(F_X(x), F_Y(y)).$$

The Sklar's theorem formalizes the idea of dissecting the dependence structure from the marginals. It applies to any joint distribution. With the two marginals fixed, any joint distribution is uniquely defined by a copula function, which “glues” together the two marginals. Based on the Sklar's theorem, there exists a copula function  $C(\cdot, \cdot)$  such that the joint risk-neutral distribution between the market return and the stock return can be expressed as  $Q_{mi} = C(Q_m(x), Q_i(y))$ . A simple change of variable gives the following<sup>12</sup>

$$\int x^\gamma h(y) dQ_{mi}(x, y) = \int_{[0,1]^2} \left[ Q_m^{-1}(u) \right]^\gamma h \left( Q_i^{-1}(v) \right) dC(u, v). \quad (6)$$

Now I can formalized the idea of bounding the term  $\mathbb{E}[h(R_i)]$ , which is equivalent to bounding the integral in (6), because the denominator in (5) can be treated as known (The marginal  $Q_m$  is recovered from the index option prices). Let  $\mathcal{C}$  be the set of all two-dimensional copula functions, my bounds are defined as follows:

$$\min_{C \in \mathcal{C}} \int_{[0,1]^2} k(u, v) dC(u, v) \leq \int x^\gamma h(y) dQ_{mi}(x, y) \leq \max_{C \in \mathcal{C}} \int_{[0,1]^2} k(u, v) dC(u, v), \quad (7)$$

where the integrand  $k(u, v)$  is fully specified as

$$k(u, v) = \left[ Q_m^{-1}(u) \right]^\gamma h \left( Q_i^{-1}(v) \right). \quad (8)$$

The integrand term absorbs all the information about the risk-neutral marginals, leaving the copula function the only unknown ingredient. This integrand is completely specified because the marginals  $Q_m$  and  $Q_i$  (as well as their inverses) are recovered from the option prices.

Calculating the two bounds in (7) is an optimization problem defined within a functional space (the space of all copula functions, as denoted by  $\mathcal{C}$ ), which makes it difficult to solve. But, if the integrand is also two-increasing like the copula function<sup>13</sup>, which holds when the payoff function

<sup>12</sup>Strictly speaking, the inverse notations for the two marginal CDFs (which might not be continuous) in (6) should be treated as generalized inverse distribution functions. That is, the notations  $Q_j^{-1}$  in equation (6) carry the following definition:  $Q_j^{-1}(p) = \inf\{x \in \mathbb{R} : Q_j(x) \geq p\}$ , for  $j \in \{m, i\}$ .

<sup>13</sup>See the definition of this concept in bullet point 3. of Definition 1.

$h$  is non-decreasing, by Corollary 2.2 of [Tchen \(1980\)](#)

$$\min_{C \in \mathcal{C}} \int_{[0,1]^2} k(u, v) \, dC(u, v) = \int_{[0,1]^2} k(u, v) \, d \left( \min_{C \in \mathcal{C}} C(u, v) \right), \quad (9)$$

$$\max_{C \in \mathcal{C}} \int_{[0,1]^2} k(u, v) \, dC(u, v) = \int_{[0,1]^2} k(u, v) \, d \left( \max_{C \in \mathcal{C}} C(u, v) \right), \quad (10)$$

where  $\min_{C \in \mathcal{C}} C(u, v)$  and  $\max_{C \in \mathcal{C}} C(u, v)$  are defined *point-wise* for any  $(u, v) \in [0, 1]^2$ . These point-wise bounds for copulas are characterized by Maurice René Fréchet and Wassily Hoeffding through the following Theorem.

**Theorem 2.** (*Fréchet-Hoeffding theorem*) *If  $C(u, v)$  is a copula, then*

$$\max(u + v - 1, 0) \leq C(u, v) \leq \min(u, v), \quad (u, v) \in [0, 1]^2.$$

One can easily verify that both the lower bound  $\max(u + v - 1, 0)$  and the upper bound  $\min(u, v)$  are copulas according to Definition 1. Thus, we can substitute the Fréchet-Hoeffding lower bound into the right hand side of (9) and the upper bound into the right hand side of (10). These arguments lead to Result 1, the key to the whole methodological framework of this paper.

**Result 1.** *If the payoff function  $h : \mathbb{R}_+ \mapsto \mathbb{R}$  is increasing, then*

$$\frac{\int_0^1 \left[ Q_m^{-1}(u) \right]^\gamma h \left( Q_i^{-1}(1 - u) \right) \, du}{\int_0^1 \left[ Q_m^{-1}(u) \right]^\gamma \, du} \leq \mathbb{E}[h(R_i)] \leq \frac{\int_0^1 \left[ Q_m^{-1}(u) \right]^\gamma h \left( Q_i^{-1}(u) \right) \, du}{\int_0^1 \left[ Q_m^{-1}(u) \right]^\gamma \, du}.$$

Sharpness of the bounds in Result 1 are due to the fact that both bounds for copula functions in the Fréchet-Hoeffding theorem are themselves copulas. The following result summarizes this property with greater details.

**Result 2.** *If the payoff function  $h$  is increasing, bounds for  $\mathbb{E}[h(R_i)]$  are sharp in the sense that*

1. *the lower bound is achievable when  $Q_i(R_i) + Q_m(R_m) = 1$ , that is, the risk-neutral stock and market returns are countermonotonic; and*
2. *the upper bound is achievable when  $Q_i(R_i) = Q_m(R_m)$ , that is, the risk-neutral stock and market returns are comonotonic<sup>14</sup>.*

Result 1 and 2 provides an analytical framework to derive sharp bounds for  $\mathbb{E}[h(R_i)]$ , when

---

<sup>14</sup>Two random variables are said to be countermonotonic if one is a monotonically decreasing transformation of the other ( $R_i = Q_i^{-1}(1 - Q_m(R_m))$  here as  $Q_i^{-1}(1 - Q_m(\cdot))$  is a decreasing function); they are said to be comonotonic if one is a monotonically increasing transformation of the other ( $R_i = Q_i^{-1}(Q_m(R_m))$  here as  $Q_i^{-1}(Q_m(\cdot))$  is an increasing function).

$h$  is monotonic<sup>15</sup>. It is worthwhile noting that, when  $h$  is not monotonic, these results does not hold because both equation (9) and (10) will become invalid. As a result, no analytical bounds are available for the expectation. In Section 4.1, I will provide a numerical solution to bounding  $\mathbb{E}[h(R_i)]$  for any well behaved payoff function  $h$ .

The (relative) risk-aversion parameter  $\gamma$  in the power utility function clearly affects the behavior of the bounds. I summarize its influences below.

**Result 3.** *If function  $h : \mathbb{R}_+ \mapsto \mathbb{R}$  is monotonic,*

1. *When  $\gamma = 0$ , the lower and the upper bounds agree and they both equal  $\mathbb{E}^*[h(R_i)]$ , the risk-neutral expectation of  $h(R_i)$ ;*
2. *For any  $0 < \gamma < \infty$ , as  $\gamma$  increases, the lower bound decreases and the upper bound increases;*
3. *If the function  $h$  is uniformly bounded, let  $h_{\min} = \inf_x h(x)$  and  $h_{\max} = \sup_x h(x)$ , then as  $\gamma \rightarrow \infty$ , the lower bound goes to  $h_{\min}$  and the upper bound goes to  $h_{\max}$ , the option-implied bounds become trivial.*

Based on Result 3, from the perspective of a risk-neutral investor, lower and upper bounds for the expectation  $\mathbb{E}[h(R_i)]$  both equal the risk-neutral one. As the investor becomes more risk-averse, the interval between the bounds becomes wider. In the extreme case of  $\gamma \rightarrow \infty$ , the bounds become totally trivial because they add no useful information to evaluating  $\mathbb{E}[h(R_i)]$ , which will always lie within  $[h_{\min}, h_{\max}]$ . For example, under the scenario that  $h(R_i) = I(R_i \leq q)$ , the bounds derived from Result 1 for the crash probability  $\mathbb{P}[R_i \leq q]$  become  $[0, 1]$  when  $\gamma$  approaches infinity.

I further simplify bounds for the crash probabilities, summarized in Result 4.

**Result 4.** *For the crash probability of a stock, we have that for all  $q \geq 0$ ,*

$$\frac{\int_0^{Q_i(q)} [Q_m^{-1}(u)]^\gamma du}{\int_0^1 [Q_m^{-1}(u)]^\gamma du} \leq \mathbb{P}[R_i \leq q] \leq \frac{\int_{1-Q_i(q)}^1 [Q_m^{-1}(u)]^\gamma du}{\int_0^1 [Q_m^{-1}(u)]^\gamma du}.$$

*In addition, the lower bound is achieved when the risk-neutral stock and market returns are comonotonic and the upper bound is achieved when the two risk-neutral returns are countermonotonic.*

Notice that for the stock crash probabilities, the way these two bounds are achieved switch from the way summarized in Result 2. This is due to the fact that  $h(R_i) = I(R_i \leq q)$  is a decreasing function. To illustrate this property under a more familiar economic setting, Result 5

<sup>15</sup>If the function  $h$  is decreasing, we can apply Result 1 to  $(-h)$  instead. And correspondingly, from Result 2, the lower bound will be achieved when the two risk-neutral returns are comonotonic, and the upper bound will be achieved when the two risk-neutral returns are countermonotonic.

below summarizes the behaviors of bounds for  $\mathbb{P}[R_i \leq q]$  in terms of risk-neutral stock betas and correlations.

**Result 5.** Denote by  $\rho_i^*$  the risk-neutral correlation between returns of stock  $i$  and the market, and define the risk-neutral beta of stock  $i$  as  $\beta_i^* = \text{cov}^*[R_m, R_i] / \text{var}^*[R_m]$ . For any  $q \geq 0$ ,

1. when  $\mathbb{P}[R_i \leq q]$  achieves the lower bound,  $\beta_i^*$  and  $\rho_i^*$  reaches their upper bounds, which must be positive;
2. when  $\mathbb{P}[R_i \leq q]$  achieves the upper bound,  $\beta_i^*$  and  $\rho_i^*$  reaches their lower bounds, which must be negative.
3. In addition, without imposing any assumptions on the dependence structure between the two returns, the lower bound of  $\rho_i^*$  can be strictly greater than minus one and the upper bound of  $\rho_i^*$  can be strictly smaller than one.

The above results tell us that, treating the risk-neutral marginals as given, the more correlated the stock and the market are (under the risk-neutral measure), the smaller the crash probability is for this stock. Comparing the two bounds for  $\mathbb{P}[R_i \leq q]$ , intuitively, the lower bound here is more likely to be closer to the “true” crash probability, because the risk-neutral stock and market returns are more likely to be positively correlated (than negatively correlation). This intuition is confirmed by the data in Section 3.1.

Now I use a very simple example to demonstrate the nice properties of the bounds, in which I assume that both the stock and the market returns are log-normal. All the bounds below are derived by applying Result 1.

**Result 6.** Assume that both of the two risk-neutral marginals are log-normal, that is,  $\log R_m \sim \mathcal{N}(\mu_m, \sigma_m^2)$  and  $\log R_i \sim \mathcal{N}(\mu_i, \sigma_i^2)$ , where  $\mu_m + \frac{1}{2}\sigma_m^2 = \mu_i + \frac{1}{2}\sigma_i^2 = \log R_f$ .

1. The risk-neutral beta of stock  $i$  must satisfy

$$\frac{e^{-\sigma_i\sigma_m} - 1}{e^{\sigma_m^2} - 1} \leq \beta_i^* \leq \frac{e^{\sigma_i\sigma_m} - 1}{e^{\sigma_m^2} - 1}.$$

2. The risk-neutral correlation between the return of stock  $i$  and the market, denoted by  $\rho_i^*$ , must be such that

$$\frac{e^{-\sigma_i\sigma_m} - 1}{\sqrt{(e^{\sigma_m^2} - 1)(e^{\sigma_i^2} - 1)}} \leq \rho_i^* \leq \frac{e^{\sigma_i\sigma_m} - 1}{\sqrt{(e^{\sigma_m^2} - 1)(e^{\sigma_i^2} - 1)}}.$$

3. The physical crash probability of stock  $i$  is bounded by

$$\Phi\left(\Phi^{-1}(p_i^*) - \gamma\sigma_m\right) \leq \mathbb{P}[R_i \leq q] \leq \Phi\left(\Phi^{-1}(p_i^*) + \gamma\sigma_m\right),$$

where

$$p_i^* = \mathbb{P}^*[R_i \leq q] = \Phi \left[ \frac{1}{\sigma_i} \log \left( \frac{q}{R_f} \right) + \frac{1}{2} \sigma_i \right]$$

is the risk-neutral crash probability,  $\Phi(\cdot)$  is the CDF of a standard normal distribution.

Even under this simple log-normal case, the benefits of resorting to the Fréchet-Hoeffding bounds are clear. The risk-neutral correlation between the two returns is mostly bounded away from one (and minus one). In Figure 2, I plot the minimum and maximum achievable  $\rho_i^*$  under different combinations of volatilities  $(\sigma_m, \sigma_i)$ . When the two returns become more volatile and different, the maximum achievable  $|\rho_i^*|$  is very far away from one.

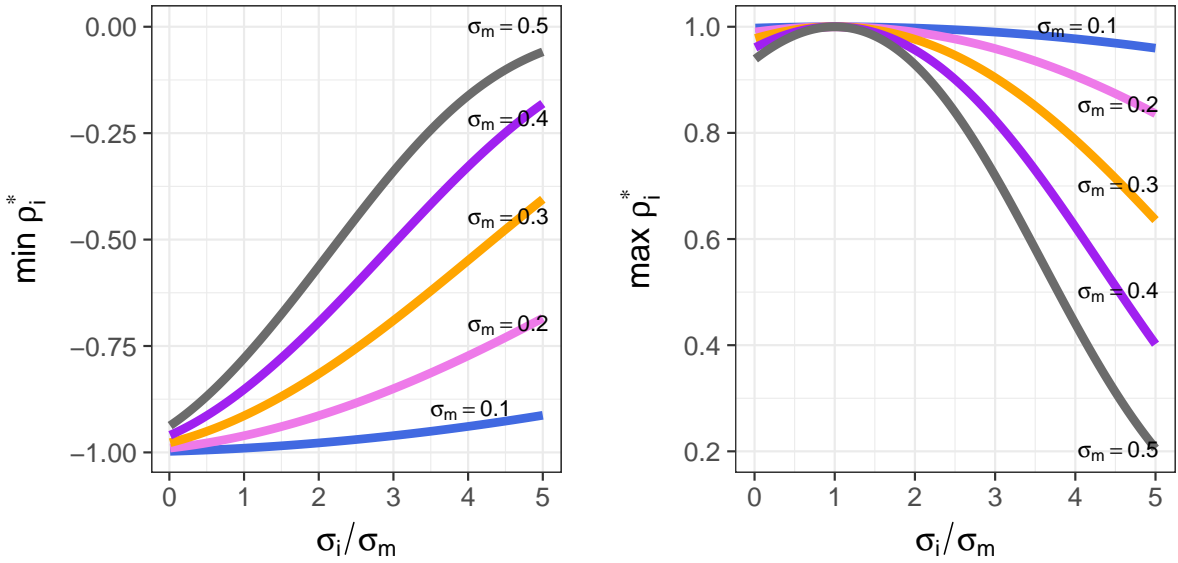


Figure 2: Bounds for the risk-neutral correlation between the market and stock returns when both are log-normal. The key point here is that under my theoretical framework, the minimum or maximum can be far away from minus one or one.

One may consider that since  $\mathbb{E}^*[R_m^\gamma h(R_i)] = \text{cov}^*[R_m^\gamma, h(R_i)] + \mathbb{E}^*[R_m^\gamma] \mathbb{E}^*[h(R_i)]$ , knowing the risk-neutral marginals (and thus, all marginal moments if they exist), the expectation can then be bounded without resorting to Result 1 because  $\text{cov}^*[R_m^\gamma, h(R_i)] \leq \sqrt{\text{var}^*[R_m^\gamma] \text{var}^*[h(R_i)]}$ . For example, for the joint log-normal example, this approach will generate the following crash probability bounds

$$p_i^* - \sqrt{p_i^*(1 - p_i^*) [\exp(\gamma^2 \sigma_m^2) - 1]} \leq \mathbb{P}[R_i \leq q] \leq p_i^* + \sqrt{p_i^*(1 - p_i^*) [\exp(\gamma^2 \sigma_m^2) - 1]}. \quad (11)$$

The key idea behind these bounds is the Cauchy-Schwartz inequality. Crash probability bounds derived in this way are not even guaranteed to fall within zero and one, and they are loose, simply

because the Cauchy-Schwartz inequality is not sharp once the marginal distributions are fixed as known. In Figure 3, I compare the behavior of crash probability bounds derived using the proposed method with bounds derived from (11). The results confirm the sharpness of the proposed bounds across various settings.

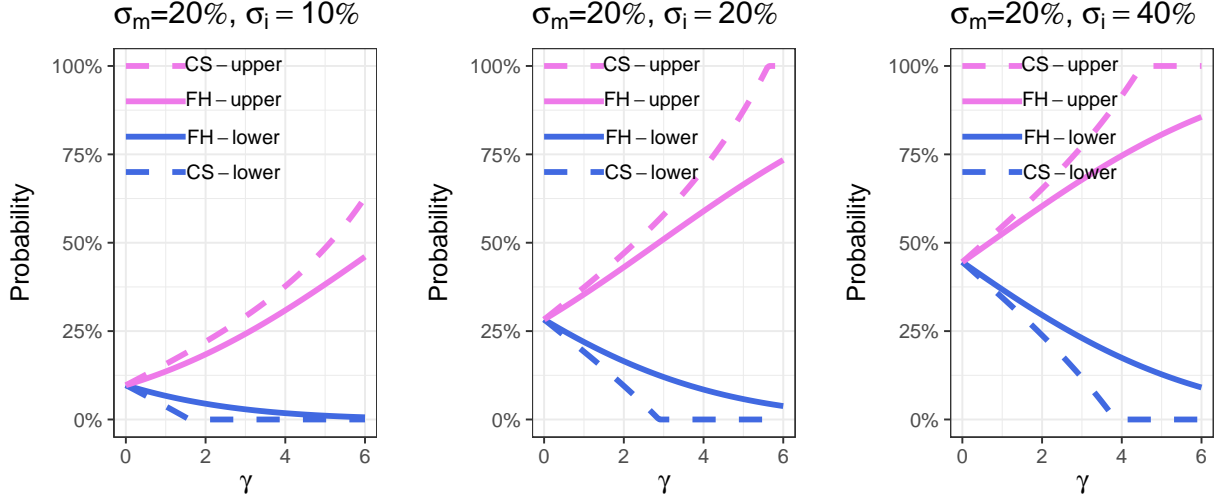


Figure 3: Comparing bounds derived from Result 1 (based on the Fréchet-Hoeffding theorem, FH for short) and bounds based on the Cauchy-Schwartz inequality (CS for short): the log-normal example of over 10% crash.

Bounds derived above are sharp without acquiring additional information (only treating the option prices on the market and the stock as known) or making specific assumptions on the dependence structure. When additional information about the copula function is available, these bounds can be improved<sup>16</sup>. However, it is not feasible here because no liquid market exists for options written on both the market and a specific stock.

### 1.3 Recovering the risk-neutral marginal distributions

In this section, I outline my approach to reconstruct risk-neutral marginals from options prices to complete the methodological framework. Let the constant  $S_0$  be the price of the underlying (e.g., a stock or the market index) today and the random variable  $S$  be the underlying asset price at maturity. Assume that the underlying asset does not pay dividend, then  $S = RS_0$  where  $R \sim Q$  is the gross return on the underlying asset;  $Q$  is the risk-neutral distribution of this gross return. Our goal is to recover  $Q$  from the prices of European options on this asset, which can be expressed

<sup>16</sup>See Tankov (2011) for some improved Fréchet-Hoeffding bounds when the prices of some options carrying information about the copula function can be used.

as

$$\text{put}(K) = \frac{1}{R_f} \int_0^\infty \max(K - xS_0, 0) dQ(x), \quad (12)$$

where  $\text{put}(K)$  denotes the price of a put option with a strike price  $K$ . Integrating (12) by parts yields:  $\int_0^{\frac{K}{S_0}} Q(x) dx = R_f \text{put}(K)/S_0$ . Taking derivatives with regard to  $K$ ,

$$Q\left(\frac{K}{S_0}\right) = R_f \text{put}'(K).$$

Combine the result above with the put-call parity, i.e.,  $\text{call}(K) - \text{put}(K) = S_0 - K/R_f$ , where  $\text{call}(K)$  represents the corresponding call option price with a strike  $K$ ,

$$Q\left(\frac{K}{S_0}\right) = R_f \text{call}'(K) + 1.$$

Throughout my execution, I only use the prices of out-of-the-money options, that is,

$$Q\left(\frac{K}{S_0}\right) = \begin{cases} R_f \text{put}'(K), & K \leq R_f S_0 \\ R_f \text{call}'(K) + 1, & K > R_f S_0 \end{cases}, \quad (13)$$

because these contracts are much more liquid ones.

In reality, prices of options are only available at a few strikes. This leads to two major difficulties recovering  $Q$  using equations in (13). First, differentiation might be inaccurate when available strikes are not dense enough. To overcome this difficulty, I fit nonparametric shape-constrained models for option prices with regard to option moneyness (Pya and Wood, 2015). This procedure leads to two benefits: 1) it rules out arbitrage across different strikes at a given maturity horizon; 2) it smoothly interpolates between strikes to enable accurate and stable differentiation in (13). Technical details of this approach are available in the Appendix.

The second difficulty is that there is not enough information about the tail of the marginal distribution, because extremely deep out-of-the-money (DOOM) options are not frequently traded. One straightforward way to deal with this issue is to extrapolate from the nonparametric fitting. However, extrapolation is known to be unstable for many nonparametric methods. Thus, I compute hypothetical DOOM option prices assuming that the volatility surface flatten out as moneyness becomes either very small or very large. This assumption has an asymptotic justification due to no arbitrage. Details of the theory and implementation are also given in the Appendix.

## 2 Data

I focus on firms included in the S&P 500 index. The index constituent data are from Compustat. The options data I use are monthly from OptionMetrics. The sample period is from January 1996



to December 2017. At the end of each month, I query the OptionMetrics database for firms that have been included to the S&P 500 index before the beginning of that year. The monthly volatility surface data of S&P 500 index option (SPX) are also collected. I keep the volatility surface data with time-to-maturity of one month, three months, six months and one year. Risk-free rates are linearly interpolated from the yield curves, provided also by OptionMetrics. Prices, returns, share volumes and shares outstanding of individual stocks are monthly from CRSP. All other firm characteristics that are used in the remaining parts of this paper come from Compustat. Table 1 provides summary statistics of the sample counts.

[Table 1 about here]

Additional concerns may rise against stocks paying dividends and the fact that individuals stock options are American-style. The use of volatility surface data from OptionMetrics can help mitigate the impacts. For all options (including the S&P 500 index option), OptionMetrics accommodates the dividend effects by projecting dividend yields from historical dividend records. For American options, OptionMetrics computes the implied volatilities through a proprietary binomial tree algorithm which accounts for the early-exercise premia. Given the relatively short maturity horizon under consideration and the use of only out-of-the-money options, the European and American implied volatility tend to be close. Thus, I take the volatility surfaces as measures of European implied volatility, following Carr and Wu (2009); Martin and Wagner (2018).

### 3 Empirical Tests

#### 3.1 In-sample tests: option-implied crash probability bounds are tight

At the end of each month, I compute the forward looking bounds for the probabilities of (gross) stock returns being less than  $q = 80\%$ ,  $90\%$  or  $95\%$ . The forecasting horizons under consideration are  $\tau = 1, 3, 6$  or  $12$  months. For stock  $i$ , I denote by  $\text{ProbLower}_{i,t}(\tau, q)$  the lower bound and by  $\text{ProbUpper}_{i,t}(\tau, q)$  the upper bound, both forecasted over horizon  $\tau$  conditioning on information at time  $t$ . The risk-aversion parameter is fixed as  $1.5$  throughout my execution<sup>17</sup>.

In report in Table 2 and 3 the summary statistics of these forecasting bounds.

[Table 2 and 3 about here]

Since the bounds are computed for each firm at the end of each month, the two tables focus on

---

<sup>17</sup>The main regression results and out-of-sample forecasts are robust against any specification from one to three. If the risk-aversion parameter is too large, the bounds become loose, according to the theoretical property in Result 3.

different aspects. Table 2 summarizes variation across firms by first averaging the bounds for each firm along the time dimension. Table 3 summarizes variation across time by first averaging the bounds for each month across all firms. Results in these tables suggest pronounced variation both across time and cross-sectionally. Across all three cases, there are more cross-sectional variation than time-series variation on average, especially for lower bound.

Denote by  $R_{i,t \rightarrow t+\tau}$  the  $\tau$  period ahead gross returns when the current time is  $t$ . To test whether these forecasting bounds are tight or not, I first run linear regressions with the following specification: for the lower bound

$$I(R_{i,t \rightarrow t+\tau} \leq q) = \alpha + \beta \text{ProbLower}_{i,t}(\tau, q) + \varepsilon_{i,t+\tau},$$

or for the upper bound

$$I(R_{i,t \rightarrow t+\tau} \leq q) = \alpha + \beta \text{ProbUpper}_{i,t}(\tau, q) + \varepsilon_{i,t+\tau},$$

with  $q = 0.80, 0.90$  and  $0.95$ . Notice that the expectations of  $I(R_{i,t \rightarrow t+\tau} \leq q)$ , that is,  $\mathbb{E}[I(R_{i,t \rightarrow t+\tau} \leq q)]$  should be the true crash probability  $\mathbb{P}[R_{i,t \rightarrow t+\tau} \leq q]$ <sup>18</sup>. If the bounds are tight, which means that they are close to the true crash probability, the parameter  $\beta$  should be close to one and  $\alpha$  should be approximately zero.

The regression results are shown in Table 4. The standard errors in parentheses are two-way cluster following Petersen (2009). The standard errors in square brackets are from block bootstrap procedures according to Martin and Wagner (2018) with 2500 simulations. The intercept parameters are mostly not significantly different from zero, specially over longer maturity horizons. The slope parameters are always significant, meaning that the bounds can explain variation in the crash probability. Most importantly, the estimates agree reasonably well with the a prior belief that  $\beta \approx 1$  and  $\alpha \approx 0$ . The slope coefficients for the lower bounds almost equal one perfectly for all four maturity horizons. The same coefficients are around 0.7 to 0.9 when the forecasting horizon is one month for the upper bound. The smallest case is when the forecasting horizon is one year, under which the slope coefficients for the upper bound are around 0.5 to 0.6. These slightly smaller regression coefficients suggest that the upper bound might not be as tight as the lower bound, which agrees with the intuition behind Result 5.

[Table 4 about here]

I also test the tightness of the bound using logistic regressions. To proceed, I first transform

---

<sup>18</sup>Both the probability and the expectation here should be conditional. I omit the time subscript for simplicity.

the bounds for probabilities to bounds to the log-odds:

$$\text{LogOddsLower}_{i,t}(\tau, q) = \log \left( \frac{\text{ProbLower}_{i,t}(\tau, q)}{1 - \text{ProbLower}_{i,t}(\tau, q)} \right),$$

$$\text{LogOddsUpper}_{i,t}(\tau, q) = \log \left( \frac{\text{ProbUpper}_{i,t}(\tau, q)}{1 - \text{ProbUpper}_{i,t}(\tau, q)} \right).$$

Then I run logistic regressions by regressing the indicators of events  $I(R_{i,t \rightarrow t+\tau} \leq q)$  on the the two bounds for log-odds. If the original bounds for probabilities are tight, the regression coefficients of the log-odds will also be close to one. I report in Table 5 the results from these logistics regressions. For most cases, except for the one with time horizon length being twelve months and  $q = 0.95$ , this regression coefficient equals almost perfectly to one. These findings further confirm the tightness of the bounds.

[Table 5 about here]

Next, I adjust for stock characteristics in the linear regression tests. Eleven characteristics are under consideration, which are rolling-window stock beta (five-year window), momentum (past twelve month return excluding the last month), (log) size, book-to-market ratio, past volatility (last one month), gross profitability over book asset, leverage (debt-to-asset), solvency (cash or cash equivalent to current liability), turnover, detrended turnover, and short interest. These characteristics are ones that have been reported to be related to expected returns (Fama and French, 1993; Jegadeesh and Titman, 1993) and crashes (Chen et al., 2001; Greenwood et al., 2018). Table 6, 7 and 8 report the regression outcomes for a crash of over 20%, 10% and 5% separately. Through these tests, the crash probability bounds stay consistently significant. Most importantly, these multivariate regressions including stock characteristics are have smaller adjusted  $R^2$  compared with the univariate case including only crash probability bounds. These evidences suggest that the option-implied bounds drive out characteristics in terms of explaining variation in the crash probabilities.

[Table 6, 7 and 8 about here]

### 3.2 Out-of-sample forecasts

The crash probability bounds rely on no free parameters, as they are observable in real time together with the security prices. This feature makes them natural candidates for out-of-sample

forecasting. In this section, I demonstrate that they do perform well forecasting crash events at the stock level, which can be done by simply thresholding the forward-looking crash probability bounds.

To pose some real challenges, I design a procedure to emulate an avid “data-snooper”. In doing so, I split the dataset into a training and a testing sample. The stock characteristics are combined through linear regressions, as well as logistic regressions, by fitting them to the training sample. In addition, when fitting these models, I select the “best” possible models through cross-validation using the LASSO.

The predictive power of forecasting bounds is then compared with the pure data-mining procedure. The forecasting target is the events of individual stock crashes. The performance measure is the ROC curve and the area under the curve (AUC) measure, which balance the type-I and type-II forecasting errors.

I report in Table 9 the AUC statistics for the option-implied bounds and the statistical procedures. The results in Table 9 confirm that simply thresholding the option-implied crash probability bounds outperform the statistical procedure combining various stock characteristics. The lower bounds consistently dominate the statistical procedures. For all approaches, the forecasting power in general is more pronounced when  $q$  becomes smaller (AUC becomes larger). Out-of-sample forecasting accuracy in general declines as the forecasting horizon becomes longer. To visualize the performances of different approach, I also plot the ROC curves for a crash over 20% in Figure 4.

[Table 9 about here]

[Figure 4 about here]

## 4 Extension and Application

### 4.1 Bounds for non-monotonic contingent payoffs

For a general function  $h$ , there is no guarantee that  $x^\gamma h(y)$  is two-increasing, which prevents us from using the Fréchet and Hoeffding bounds for solving the optimization problem defined in (7).

Hofer and Iacò (2014) propose an algorithm to solve this problem. For any well-behaved<sup>19</sup> function  $k$  in (7),

$$\max_{C \in \mathcal{C}} \int_{[0,1]^2} k(u, v) \, dC(u, v) \approx \max_{\pi \in \mathcal{P}_n} \frac{1}{n} \sum_{i=1}^n k\left(\frac{i}{n+1}, \frac{\pi(i)}{n+1}\right), \quad \text{as } n \text{ is large enough,} \quad (14)$$

where  $\mathcal{P}_n$  is the set of all possible permutations (the total number of which is  $n!$ ) of the set  $\{1, \dots, n\}$ ;  $\pi \in \mathcal{P}_n$  selects one specific permutation of  $\{1, \dots, n\}$ , that is,  $\pi$  is a one-to-one mapping from the  $n$ -elements to themselves. The right-hand side of (14) is a canonical problem in combinatorial optimization called the linear assignment problem<sup>20</sup>. Algorithmic solution to this problem is due to Kuhn (1955), which is called the Hungarian algorithm. This algorithm reduces the complexity of solving the right-hand side optimization problem in (14) from  $O(n!)$  (brute-force searching) to  $O(n^3)$ .

In terms of the lower bounds, one can apply the Hungarian algorithm to the integral involving  $-k(u, v)$  to get an upper bound. The negative of the upper bound for  $\int_{[0,1]^2} [-k(u, v)] \, dC(u, v)$  minimizes the original integral over the space of copula functions.

Applying the Sklar's theorem and the methods presented above gives us the following result:

**Result 7.** *Let  $h$  be a function that is continuous almost everywhere. Define function  $k(u, v)$  on  $[0, 1]^2$  as in equation (8). Let  $\pi_{\min}$  be a permutation of  $\{1, \dots, n\}$  that minimizes  $\sum_{k=1}^n k\left(\frac{i}{n+1}, \frac{\pi(i)}{n+1}\right)$ , and  $\pi_{\max}$  be a permutation of  $\{1, \dots, n\}$  that maximizes  $\sum_{k=1}^n k\left(\frac{i}{n+1}, \frac{\pi(i)}{n+1}\right)$ , then*

$$\frac{1}{nC} \sum_{i=1}^{n+1} k\left(\frac{i}{n+1}, \frac{\pi_{\min}(i)}{n+1}\right) \leq \mathbb{E}[h(R_i)] \leq \frac{1}{nC} \sum_{i=1}^{n+1} k\left(\frac{i}{n+1}, \frac{\pi_{\max}(i)}{n+1}\right),$$

*holds approximately for  $n$  being large enough, where the constant  $C$  equals  $\int_0^1 [Q_m^{-1}(u)]^\gamma \, du$ .*

Result 7 is valid for a very general class of functions. One simple but important example is when  $h(R_i) = I(q_1 \leq R_i \leq q_2)$ , that is, when we are interested in evaluating the probability that stock  $i$ 's return falls in the interval  $[q_1, q_2]$ .

## 4.2 Fragility and stability measures of the global banking system

Baron et al. (2018) report the link between the large declines in bank equity and macroeconomic downturn, as well as the predicative power of large bank equity declines on banking crisis. Since the bank equity returns can only be calculated *ex post*, the forward-looking equity crash bounds that I have introduced in this paper is a clear *ex ante* alternative to consider.

<sup>19</sup>Here, it means that: 1) the function guarantees that the integral is finite; 2) the function is continuous almost everywhere within its domain.

<sup>20</sup>See Burkard et al. (2012) for an extensive coverage on this topic

In this section, I demonstrate a specific application of the derived bounds to monitoring the crash probability of global systemically important banks (G-SIBs), and construct two global banking fragility measures from the crash probability bounds.

The G-SIBs under consideration are listed in Table 12. Twenty-one G-SIBs that have been included by the Financial Stability Board since 2011 are considered. These chosen G-SIBs all have their stocks traded in the US stock market or have issued American depositary receipts. Banks that are not traded in the US stock market are not considered in this study. Table 12 also reports the time periods during which option data are available for the equity of these banks.

I compute the forward-looking crash probability bounds for the equity value of these global banks using the method described in Section 1. Then I define two aggregate measures using these bounds for individual banks to monitor their overall fragility. For a given set of banks, the probability of *at least* one crash can be bounded from below as follows:

$$\begin{aligned}\mathbb{P} [\text{at least one crash}] &= \mathbb{P} [\cup_i \{R_i \leq q\}] \\ &\geq \max_i \mathbb{P}[R_i \leq q] \\ &\geq \max_i \inf \mathbb{P}[R_i \leq q],\end{aligned}$$

where  $q$  is a pre-specified return level (for example, 80%) to define a crash (large equity decline),  $\inf \mathbb{P}[R_i \leq q]$  is the lower bound for the crash probability derived from option data for individual bank  $i$ . I define the quantity,  $\max_i \inf \mathbb{P}[R_i \leq q]$ , as the *fragility* measure: the higher this measure is, the more likely that a banking crisis will emerge. On the other hand, for the same set of banks, the probability that all of them are facing large equity value declines is bounded from above because

$$\begin{aligned}\mathbb{P} [\text{all crash}] &= \mathbb{P} [\cap_i \{R_i \leq q\}] \\ &\leq \min_i \mathbb{P}[R_i \leq q] \\ &\leq \min_i \sup \mathbb{P}[R_i \leq q],\end{aligned}$$

then the probability of *no* system-wide crash is bounded from below:

$$1 - \mathbb{P} [\text{all crash}] \geq 1 - \min_i \sup \mathbb{P}[R_i \leq q],$$

where  $\sup \mathbb{P}[R_i \leq q]$  is the upper bound for the crash of bank  $i$ . I define  $1 - \min_i \sup \mathbb{P}[R_i \leq q]$  as a measure of *stability*: if this quantity is large, the probability of a full-scale melt down of the global banking system will be small.

I show in Figure 5 these two measures over the one-year horizon. The crash events is defined by specifying  $q$  as 0.80 (a 20% crash), 0.70 (a 30% crash) and 0.60 (a 40% crash). The time scale is monthly from January 1996 to December 2017. The two measures move in opposite direction as expected. The fragility measure surges and the stability measure plunges during the period of subprime crisis. The stability measure *begins* to decline from mid 2007, which predates the onset of the crisis.

[Figure 5 about here]

### 4.3 An Upper Bound for the Expected Return of a Stock and the CVIX index

In this section, I introduce an upper bound for the expected return of a stock in the eyes of a log investor holding the market portfolio. Consider a special case of result one when  $\gamma = 1$  and  $h(y) = y$ , then

$$\begin{aligned}\mathbb{E}[R_i] &\leq \frac{\int_0^1 Q_m^{-1}(u) Q_i^{-1}(u) du}{\int_0^1 Q_m^{-1}(u) du} \\ &= \frac{\int x Q_i^{-1}(Q_m(x)) dQ_m(x)}{\int x dQ_m(x)} \\ &= \frac{\mathbb{E}^*[R_m Q_i^{-1}(Q_m(R_m))]}{R_f} \\ &= \frac{\mathbb{E}^*[g(S_m)]}{R_f},\end{aligned}$$

where  $S_m$  represents market level at the end of the forecasting horizon, and function  $g$  is defined based on the two risk-neutral marginals as well as the current market price  $S_{m,0}$  as

$$g(x) = \frac{x}{S_{m,0}} Q_i^{-1} \left( Q_m \left( \frac{x}{S_{m,0}} \right) \right).$$

Apply the Carr-Madan formula (Carr and Madan, 1998), take the risk-neutral expectations on both sides, and change the order of double integrals,

$$\frac{\mathbb{E}^*[g(S_m)]}{R_f} = \frac{g(F_m)}{R_f} + \int_0^{F_m} g''(K) \text{put}(K) dK + \int_{F_m}^{\infty} g''(K) \text{call}(K) dK,$$

where  $\text{call}(K)$  and  $\text{put}(K)$  are the prices of S&P 500 index options with a strike price  $K$ , maturing at the end of the forecasting horizon;  $F_m = S_{0,m} R_f$  is the forward of the S&P 500. Thus, one can

show that

$$\begin{aligned} \mathbb{E}[R_i] &\leq Q_i^{-1}(Q_m(R_f)) \\ &\quad + \int_0^{F_m} \left[ \frac{K}{S_{m,0}} Q_i^{-1} \left( Q_m \left( \frac{K}{S_{m,0}} \right) \right) \right]'' \text{put}(K) dK + \int_{F_m}^{\infty} \left[ \frac{K}{S_{m,0}} Q_i^{-1} \left( Q_m \left( \frac{K}{S_{m,0}} \right) \right) \right]'' \text{call}(K) dK. \end{aligned} \quad (15)$$

If the forecasting horizon under consideration ends  $T$  periods ahead, we can define an index named the *comonotonic* volatility index (CVIX) for stock  $i$  as

$$\begin{aligned} \text{CVIX}_{i,T} &= \frac{1}{R_f T} \left\{ \int_0^{F_m} \left[ \frac{K}{S_{m,0}} Q_i^{-1} \left( Q_m \left( \frac{K}{S_{m,0}} \right) \right) \right]'' \text{put}(K) dK \right. \\ &\quad \left. + \int_{F_m}^{\infty} \left[ \frac{K}{S_{m,0}} Q_i^{-1} \left( Q_m \left( \frac{K}{S_{m,0}} \right) \right) \right]'' \text{call}(K) dK \right\}, \end{aligned} \quad (16)$$

and the expected return on stock  $i$  would satisfy

$$\frac{\mathbb{E}[R_i]}{TR_f} \leq \frac{Q_i^{-1}(Q_m(R_f))}{TR_f} + \text{CVIX}_{i,T}. \quad (17)$$

After recovering the risk-neutral marginals using methods in section 1.3, the CVIX index can be calculated using the prices of index options.

At the end of each month, I compute, for each individual stock, the annualized CVIX index using their option prices and the prices of index options. The forecasting horizons under consideration are  $\tau = 1, 3, 6$  or 12 months (i.e.,  $T$  in equation (16) and inequality (17) equals 1/12, 1/4, 1/2 or 1). Denoted by  $\text{CVIX}_{i,t}(T)$  the index at time  $t$  concerning  $T = \tau/12$  periods ahead. In Table 10, I report the summary statistics for the annualized CVIX. Results in these tables suggest pronounced variation both across time and cross-sectionally. CVIXs are larger for short horizons.

If the upper bound in inequality (17) is tight, we can regress the  $\tau R_{i,t \rightarrow t+\tau} / R_f$  on  $\text{CVIX}_{i,t}(T)$ , where  $\tau = 12T$  by estimating

$$\frac{\tau R_{i,t \rightarrow t+\tau}}{R_f} = \alpha + \beta \text{CVIX}_{i,t}(T) + \epsilon_{i,t+\tau},$$

and get  $\beta$  close to one. In addition, because  $\alpha$  represents the term  $\frac{Q_i^{-1}(Q_m(R_f))}{TR_f}$  in inequality (17), which should be time-varying (both the risk-free rate and the two risk-neutral marginals vary across time), I also fit a linear model with time-fixed effect,

$$\frac{\tau R_{i,t \rightarrow t+\tau}}{R_f} = \alpha_t + \beta \text{CVIX}_{i,t}(T) + \epsilon_{i,t+\tau}.$$

Specifically, for each of the four forecasting horizons, I run the two panel regressions above. When



$\tau$  is greater than one, the dependent variables clearly have overlapping components, suggesting time-series correlations. In addition, co-movement of stock returns implies the existence of cross-sectional correlations. I deal with these issues for inference by calculating two-way clustered standard errors. I also perform the block bootstrap with 2,500 replications, following the algorithm of [Martin and Wagner \(2018\)](#).

Table 11 reports the regression results for these two sets of regressions. For simple linear regressions, the  $\beta$  coefficients are mostly around 0.6 except for the case in which the time horizon is six months ( $\beta = 1.062$  in this case). For linear fixed-effect regressions, the  $\beta$  coefficients are either mildly higher or very close to one. These results suggest that the bound appear to be tight, which corroborates the accuracy of the theory and the calculation.

## 5 Conclusion

This paper has proposed a new framework to derived bounds for the expectation of a payoff that is contingent on an individual stock return. The bounds are computed directly from option prices and are forward-looking by nature. The sharpness of these bounds are theoretically guaranteed. The framework is general enough and may be of interest by itself.

Applying this framework, I compute bounds for the stock crash probabilities. Through panel regressions, I show that these crash probability bounds are close to the true crash probabilities. Out-of-sample analysis shows that they perform well in forecasting crash events and consistently outperform the combination of various stock characteristics.

At the micro-level, these bounds can provide real-time monitoring of crash risks at the firm level. Compared with a point forecast, having a forecasting bounds can be beneficial in that forecasting uncertainties are quantified and sensitivity analysis based on crash probabilities can be guided.

These crash probability bounds are potentially useful for constructing forward-looking macroeconomic indicators through thoughtful aggregation. For example, when applied to the study of G-SIBs, the maximum of the lower bounds and the minimum of the upper bounds can be used to construct fragility and stability measures of the global banking system.

## References

- Aït-Sahalia, Y. and A. W. Lo (1998). Nonparametric estimation of state-price densities implicit in financial asset prices. *Journal of Finance* 53(2), 499–547.
- Andersen, T. G., L. Benzoni, and J. Lund (2002). An empirical investigation of continuous-time equity return models. *Journal of Finance* 57(3), 1239–1284.
- Andersen, T. G., T. Bollerslev, F. X. Diebold, and H. Ebens (2001). The distribution of realized stock return volatility. *Journal of Financial Economics* 61(1), 43–76.
- Ang, A., J. Chen, and Y. Xing (2006). Downside risk. *Review of Financial Studies* 19(4), 1191–1239.
- Baron, M., E. Verner, and W. Xiong (2018). Bank equity and banking crises. *Working paper*.
- Bates, D. S. (1991). The crash of '87: Was it expected? the evidence from options markets. *Journal of Finance* 46(3), 1009–1044.
- Bernardo, A. E. and O. Ledoit (2000). Gain, loss, and asset pricing. *Journal of Political Economy* 108(1), 144–172.
- Boyer, B., T. Mitton, and K. Vorkink (2009). Expected idiosyncratic skewness. *Review of Financial Studies* 23(1), 169–202.
- Breeden, D. T. and R. H. Litzenberger (1978). Prices of state-contingent claims implicit in option prices. *Journal of Business* 51(4), 621–651.
- Breiman, L. (1960). Investment policies for expanding businesses optimal in a long-run sense. *Naval Research Logistics* 7(4), 647–651.
- Burkard, R., M. Dell'Amico, and S. Martello (2012). *Assignment Problems: Revised Reprint*. SIAM.
- Carr, P. and D. B. Madan (1998). Towards a theory of volatility trading. In R. A. Jarrow (Ed.), *Volatility: New estimation techniques for pricing derivatives*, Chapter 29, pp. 417–427. Risk Books.
- Carr, P. and L. Wu (2009). Variance risk premiums. *Review of Financial Studies* 22(3), 1311–1341.
- Chen, J., H. Hong, and J. C. Stein (2001). Forecasting crashes: Trading volume, past returns, and conditional skewness in stock prices. *Journal of financial Economics* 61(3), 345–381.
- Cochrane, J. H. and J. Saá-Requejo (2000). Beyond arbitrage: Good-deal asset price bounds in incomplete markets. *Journal of Political Economy* 108(1), 79–119.
- Constantinides, G. M., J. C. Jackwerth, and S. Perrakis (2008). Mispricing of S&P 500 index options. *Review of Financial Studies* 22(3), 1247–1277.
- Fama, E. F. and K. R. French (1993). Common risk factors in the returns on stocks and bonds. *Journal of Financial Economics* 33(1), 3–56.
- Greenwood, R., A. Shleifer, and Y. You (2018). Bubbles for Fama. *Journal of Financial Economics*.

- Hofer, M. and M. R. Iacò (2014). Optimal bounds for integrals with respect to copulas and applications. *Journal of Optimization Theory and Applications* 3, 999–1011.
- Jackwerth, J. C. and M. Rubinstein (1996). Recovering probability distributions from option prices. *Journal of Finance* 51(5), 1611–1631.
- Jegadeesh, N. and S. Titman (1993). Returns to buying winners and selling losers: Implications for stock market efficiency. *Journal of Finance* 48(1), 65–91.
- Kelly, B. and H. Jiang (2014). Tail risk and asset prices. *Review of Financial Studies* 27(10), 2841–2871.
- Kuhn, H. W. (1955). The Hungarian method for the assignment problem. *Naval Research Logistics* 2(1-2), 83–97.
- Latane, H. A. (1959). Criteria for choice among risky ventures. *Journal of Political Economy* 67(2), 144–155.
- Martin, I. (2017). What is the expected return on the market? *Quarterly Journal of Economics* 132(1), 367–433.
- Martin, I. (2018). Options and the gamma knife. *Journal of Portfolio Management* 44(6), 47–55.
- Martin, I. and C. Wagner (2018). What is the expected return on a stock? *Journal of Finance (Forthcoming)*.
- McFadden, D. (1974). Conditional logit analysis of qualitative choice behaviour. In P. Zarembka (Ed.), *Frontiers in Econometrics*. Academic Press.
- Nelsen, R. B. (2007). *An Introduction to Copulas*. Springer Science & Business Media.
- Petersen, M. A. (2009). Estimating standard errors in finance panel data sets: Comparing approaches. *Review of Financial Studies* 22(1), 435–480.
- Pya, N. and S. N. Wood (2015). Shape constrained additive models. *Statistics and Computing* 25(3), 543–559.
- Ross, S. A. (1976). Options and efficiency. *Quarterly Journal of Economics* 90(1), 75–89.
- Rubinstein, M. (1994). Implied binomial trees. *Journal of Finance* 49(3), 771–818.
- Sklar, A. (1959). Fonctions de répartition à  $n$  dimensions et leurs marges. *Publ. Inst. Statist. Univ. Paris* 8, 229–231.
- Tankov, P. (2011). Improve Fréchet bounds and model-free pricing of multi-asset options. *Journal of Applied Probability* 48(2), 389–403.
- Tchen, A. H. (1980). Inequalities for distributions with given marginals. *Annals of Probability* 8(4), 814–827.
- Tibshirani, R. (1996). Regression shrinkage and selection via the lasso. *Journal of the Royal Statistical Society, Series B*, 267–288.

Table 1: Sample Summary

This table summarizes the data sources. The sample period is monthly from January 1996 to December 2017. For each months, I query the OptionMetrics database for firms that have been included to the S&P 500 index before the beginning of that year. The data I use are the implied volatility surface data from which I collect the (implied) option premiums and corresponding strike prices. The time horizons, i.e., the date to maturity are one month, two months, six months and one year. The total number of firm-month pairs, unique firms, unique months, and the median and mean of average number of firms per month are reported. .

Maturity	1	3	6	12
Total no. of observations	128,259	127,540	126,472	126,470
No. of sample months	264	264	264	264
No. of sample firms	1033	1032	1029	1029
Median no. of firms/month	485	484	480	480
Average no. of firms/month	486	483	479	479

Table 2: Variation of crash probability bounds across firms

This table presents the summary statistics of time-series averages of crash probability bounds. The sample period is monthly from January 1996 to December 2017. The crash probabilities under consideration are  $\mathbb{P}_t[R_i \leq q]$  for  $q = 0.80, 0.90, 0.95$ . The time-series averages are taken for each firm separately. To rule out the impact of outliers, the time-series average is taken and reported only for firms with over four-year observations. Maturity horizons are one month, two months, six months and one year.

Maturity	Lower bound				Upper bound			
	1	3	6	12	1	3	6	12
No. of firms	700	699	695	695	700	699	695	695
Panel A: $q = 0.80$ , down by over 20%								
Min.	0.003	0.017	0.031	0.046	0.012	0.042	0.078	0.130
1st Qu.	0.015	0.051	0.083	0.110	0.032	0.097	0.172	0.271
Median	0.025	0.072	0.110	0.141	0.046	0.130	0.214	0.317
3rd Qu.	0.038	0.098	0.141	0.174	0.064	0.165	0.257	0.364
Max.	0.145	0.240	0.292	0.340	0.196	0.344	0.440	0.557
Mean	0.031	0.080	0.116	0.146	0.053	0.138	0.220	0.320
Std.dev.	0.023	0.040	0.047	0.050	0.031	0.056	0.068	0.074
Panel B: $q = 0.90$ , down by over 10%								
Min.	0.031	0.066	0.091	0.103	0.051	0.121	0.187	0.244
1st Qu.	0.077	0.147	0.182	0.200	0.114	0.229	0.312	0.397
Median	0.105	0.182	0.217	0.232	0.147	0.272	0.357	0.441
3rd Qu.	0.135	0.217	0.252	0.265	0.184	0.316	0.398	0.480
Max.	0.295	0.360	0.379	0.402	0.358	0.468	0.534	0.618
Mean	0.112	0.186	0.220	0.234	0.155	0.276	0.357	0.439
Std.dev.	0.047	0.054	0.052	0.050	0.057	0.067	0.066	0.065
Panel C: $q = 0.95$ , down by over 5%								
Min.	0.104	0.166	0.174	0.170	0.139	0.240	0.292	0.330
1st Qu.	0.191	0.248	0.265	0.260	0.247	0.348	0.410	0.473
Median	0.223	0.280	0.295	0.290	0.282	0.385	0.446	0.508
3rd Qu.	0.257	0.310	0.323	0.318	0.320	0.420	0.478	0.540
Max.	0.389	0.426	0.425	0.436	0.456	0.536	0.583	0.647
Mean	0.227	0.282	0.296	0.290	0.286	0.386	0.446	0.507
Std.dev.	0.050	0.047	0.044	0.044	0.056	0.054	0.052	0.053

Table 3: Variation of crash probability bounds over time

This table presents summary statistics of the cross-sectional averages of crash probability bounds. The sample period is monthly from January 1996 to December 2017. The sample period is monthly from January 1996 to December 2017. The crash probabilities under consideration are  $\mathbb{P}_t[R_i \leq q]$  for  $q = 0.80, 0.90, 0.95$ . The cross-sectional averages are take year by year. Maturity horizons are one month, two months, six months and one year.

Maturity	Lower bound				Upper bound			
	1	3	6	12	1	3	6	12
No. of months	264	264	264	264	264	264	264	264
Panel A: $q = 0.80$ , down by over 20%								
Min.	0.003	0.031	0.061	0.103	0.012	0.052	0.110	0.189
1st Qu.	0.014	0.049	0.086	0.120	0.026	0.083	0.146	0.238
Median	0.019	0.061	0.100	0.133	0.034	0.105	0.186	0.288
3rd Qu.	0.038	0.097	0.131	0.158	0.065	0.176	0.273	0.379
Max.	0.126	0.176	0.197	0.216	0.245	0.410	0.517	0.633
Mean	0.028	0.075	0.111	0.142	0.049	0.131	0.212	0.313
Std.dev.	0.022	0.033	0.033	0.029	0.037	0.066	0.079	0.088
Panel B: $q = 0.90$ , down by over 10%								
Min.	0.039	0.122	0.173	0.197	0.057	0.168	0.249	0.316
1st Qu.	0.076	0.152	0.194	0.215	0.101	0.215	0.293	0.375
Median	0.092	0.168	0.205	0.224	0.126	0.246	0.331	0.418
3rd Qu.	0.135	0.211	0.236	0.243	0.189	0.327	0.414	0.497
Max.	0.219	0.280	0.298	0.302	0.371	0.508	0.598	0.691
Mean	0.106	0.181	0.216	0.232	0.148	0.270	0.352	0.436
Std.dev.	0.041	0.038	0.030	0.023	0.062	0.071	0.072	0.075
Panel C: $q = 0.95$ , down by over 5%								
Min.	0.139	0.240	0.262	0.256	0.170	0.298	0.351	0.395
1st Qu.	0.193	0.260	0.279	0.276	0.234	0.335	0.396	0.457
Median	0.212	0.269	0.288	0.286	0.263	0.364	0.425	0.491
3rd Qu.	0.250	0.292	0.302	0.298	0.326	0.428	0.491	0.556
Max.	0.319	0.360	0.360	0.349	0.450	0.560	0.639	0.719
Mean	0.221	0.278	0.293	0.289	0.279	0.382	0.443	0.505
Std.dev.	0.038	0.026	0.021	0.019	0.059	0.057	0.059	0.064

Table 4: Tightness of the crash probability bounds: linear regression tests

This table reports the results from regressing the indicator function of realized equity returns being less than a threshold,  $q$ , on the option-implied bounds,  $\text{ProbLower}_{i,t}(\tau, q)$  and  $\text{ProbUpper}_{i,t}(\tau, q)$ , for firms belonging to the S&P 500 index. The data are monthly from January 1996 to December 2017. The return horizons, denoted by  $\tau$ , are one month, three month, six months, and one year. Results in Panel A, B, C are from the linear regressions,

$$I(R_{i,t \rightarrow t+\tau} \leq q) = \alpha + \beta \text{ProbLower}_{i,t}(\tau, q) + \varepsilon_{i,t+\tau},$$

or

$$I(R_{i,t \rightarrow t+\tau} \leq q) = \alpha + \beta \text{ProbUpper}_{i,t}(\tau, q) + \varepsilon_{i,t+\tau},$$

with  $q = 0.80, 0.90$  and  $0.95$ . Values in parentheses are standard errors with two-way clustering following [Petersen \(2009\)](#). Values in square brackets are standard errors from block bootstrap using 2500 bootstrap samples following [Martin and Wagner \(2018\)](#). Adjusted  $R^2$ s are also reported.

Maturity	Lower bound				Upper bound			
	1	3	6	12	1	3	6	12
Panel A: $q = 0.80$ , down by over 20%								
$\alpha$	−0.005 (0.002) [0.002]	−0.014 (0.005) [0.009]	−0.021 (0.008) [0.015]	−0.045 (0.009) [0.025]	−0.011 (0.003) [0.004]	−0.017 (0.007) [0.008]	−0.017 (0.012) [0.022]	−0.051 (0.016) [0.036]
$\beta$	1.034 (0.136) [0.129]	1.152 (0.105) [0.162]	1.193 (0.097) [0.177]	1.105 (0.085) [0.170]	0.703 (0.104) [0.117]	0.680 (0.076) [0.094]	0.602 (0.074) [0.151]	0.519 (0.065) [0.145]
$R^2\text{-Adj.}$	6.88%	6.84%	5.90%	5.31%	6.67%	6.08%	4.46%	3.99%
Panel B: $q = 0.90$ , down by over 10%								
$\alpha$	−0.023 (0.007) [0.008]	−0.039 (0.011) [0.011]	−0.063 (0.015) [0.039]	−0.068 (0.018) [0.060]	−0.031 (0.009) [0.010]	−0.041 (0.017) [0.026]	−0.044 (0.026) [0.046]	−0.068 (0.033) [0.076]
$\beta$	1.121 (0.093) [0.082]	1.165 (0.079) [0.121]	1.257 (0.081) [0.203]	1.195 (0.081) [0.211]	0.861 (0.084) [0.069]	0.791 (0.079) [0.143]	0.717 (0.086) [0.194]	0.634 (0.087) [0.213]
$R^2\text{-Adj.}$	7.05%	5.02%	4.27%	3.45%	7.04%	4.64%	3.22%	2.60%
Panel C: $q = 0.95$ , down by over 5%								
$\alpha$	−0.037 (0.016) [0.017]	−0.049 (0.021) [0.029]	−0.080 (0.026) [0.045]	−0.021 (0.028) [0.059]	−0.045 (0.022) [0.026]	−0.042 (0.037) [0.043]	−0.034 (0.046) [0.087]	−0.009 (0.051) [0.107]
$\beta$	1.129 (0.083) [0.088]	1.144 (0.078) [0.088]	1.239 (0.087) [0.145]	1.051 (0.092) [0.178]	0.923 (0.090) [0.092]	0.813 (0.104) [0.118]	0.717 (0.112) [0.214]	0.578 (0.108) [0.202]
$R^2\text{-Adj.}$	3.99%	2.54%	2.42%	1.77%	4.10%	2.35%	1.71%	1.26%

Table 5: Tightness of the crash probability bounds: logistic regression tests

This table reports the results from the logistic regression tests of

$$\mathbb{P}[R_{i,t \rightarrow t+\tau} \leq q] = \frac{\exp(\alpha + \beta \text{LogOddsLower}_{i,t}(\tau, q))}{1 + \exp(\alpha + \beta \text{LogOddsLower}_{i,t}(\tau, q))},$$

or

$$\mathbb{P}[R_{i,t \rightarrow t+\tau} \leq q] = \frac{\exp(\alpha + \beta \text{LogOddUpper}_{i,t}(\tau, q))}{1 + \exp(\alpha + \beta \text{LogOddUpper}_{i,t}(\tau, q))},$$

for firms belonging to the S&P 500 index, where the “LogOdds” bounds are monotonically transform from “Prob” bounds as  $\text{Prob}/(1-\text{Prob})$ . The data are monthly from January 1996 to December 2017. The return horizons, denoted by  $\tau$ , are one month, three month, six months, and one year. Values in square brackets are standard errors from block bootstrap using 2500 bootstrap samples following [Martin and Wagner \(2018\)](#). Adjusted McFadden’s pseudo- $R^2$ s are also reported ([McFadden, 1974](#)).

Maturity	Lower bound				Upper bound			
	1	3	6	12	1	3	6	12
Panel A: $q = 0.80$ , down by 20%								
$\alpha$	0.232 [0.277]	0.408 [0.302]	0.416 [0.310]	0.311 [0.277]	−0.023 [0.253]	−0.476 [0.223]	−0.782 [0.303]	−1.330 [0.212]
$\beta$	1.148 [0.099]	1.206 [0.123]	1.218 [0.136]	1.362 [0.180]	1.342 [0.089]	1.153 [0.101]	1.031 [0.187]	1.065 [0.228]
$R^2$ -Adj.	17.88%	11.35%	7.99%	7.01%	18.60%	10.58%	6.62%	5.59%
Panel B: $q = 0.90$ , down by 10%								
$\alpha$	0.383 [0.138]	0.281 [0.172]	0.340 [0.174]	0.199 [0.223]	−0.119 [0.138]	−0.509 [0.170]	−0.759 [0.221]	−1.140 [0.176]
$\beta$	1.264 [0.056]	1.243 [0.092]	1.315 [0.129]	1.294 [0.184]	1.269 [0.079]	1.106 [0.118]	0.992 [0.194]	0.895 [0.258]
$R^2$ -Adj.	10.47%	5.53%	4.18%	3.30%	10.48%	5.18%	3.26%	2.48%
Panel C: $q = 0.95$ , down by 5%								
$\alpha$	0.175 [0.146]	0.119 [0.148]	0.179 [0.155]	0.012 [0.197]	−0.265 [0.066]	−0.544 [0.120]	−0.745 [0.105]	−0.955 [0.157]
$\beta$	1.190 [0.130]	1.177 [0.092]	1.266 [0.152]	1.047 [0.227]	1.127 [0.067]	0.975 [0.122]	0.852 [0.174]	0.661 [0.189]
$R^2$ -Adj.	3.98%	2.21%	2.01%	1.44%	4.06%	2.06%	1.43%	0.99%



Table 6: Tightness of the crash probability bounds: linear regression tests adding characteristics for a 20% crash

This table reports the results from regressing the indicator function of realized equity returns being less than 0.80 on the option-implied bounds as well as other characteristics for firms belonging to the S&P 500 index. The data are monthly from January 1996 to December 2017. The return horizons are one month, three month, six months, and one year. Values in parentheses are standard errors with two-way clustering following Petersen (2009). Adjusted  $R^2$ s are also reported.

Maturity	Lower bound				Upper bound			
	1	3	6	12	1	3	6	12
intercept	0.009 (0.024)	0.077 (0.051)	0.079 (0.068)	0.093 (0.069)	-0.0004 (0.025)	0.072 (0.053)	0.094 (0.069)	0.094 (0.069)
<b>bounds</b>	0.809*** (0.116)	0.948*** (0.126)	1.277*** (0.142)	1.054*** (0.126)	0.535*** (0.109)	0.452*** (0.082)	0.451*** (0.084)	0.335*** (0.069)
beta	0.0003 (0.007)	-0.008 (0.017)	-0.040 (0.026)	-0.049* (0.027)	0.007 (0.007)	0.016 (0.016)	0.016 (0.024)	0.018 (0.024)
mom	-0.008* (0.004)	-0.007 (0.011)	0.003 (0.015)	0.001 (0.015)	-0.006 (0.004)	-0.005 (0.011)	0.007 (0.015)	0.006 (0.015)
logsize	-0.0001 (0.001)	-0.003 (0.003)	-0.001 (0.004)	-0.003 (0.004)	-0.0003 (0.001)	-0.005 (0.003)	-0.005 (0.004)	-0.006 (0.004)
bm	-0.010*** (0.003)	-0.021*** (0.007)	-0.042*** (0.009)	-0.042*** (0.009)	-0.009*** (0.003)	-0.017** (0.007)	-0.036*** (0.010)	-0.036*** (0.010)
past_vol	0.022 (0.014)	0.031 (0.029)	-0.039 (0.039)	0.023 (0.039)	0.018 (0.012)	0.056** (0.022)	0.027 (0.039)	0.064 (0.039)
gross_prof	-0.010** (0.004)	-0.019* (0.011)	-0.037** (0.017)	-0.038** (0.017)	-0.010** (0.004)	-0.017 (0.011)	-0.031* (0.018)	-0.030* (0.018)
debt/asset	-0.001 (0.004)	-0.011 (0.011)	-0.042** (0.019)	-0.048** (0.019)	0.001 (0.004)	-0.008 (0.012)	-0.037* (0.020)	-0.040** (0.020)
cce/cliab.	-0.002** (0.001)	-0.005** (0.002)	-0.010*** (0.003)	-0.011*** (0.003)	-0.002* (0.001)	-0.004* (0.002)	-0.008** (0.003)	-0.009** (0.003)
turnover	0.029 (0.050)	-0.017 (0.108)	0.012 (0.133)	0.072 (0.134)	0.020 (0.050)	-0.003 (0.110)	0.050 (0.135)	0.070 (0.134)
d_turnover	0.023 (0.060)	0.141 (0.133)	0.281 (0.184)	0.165 (0.183)	0.038 (0.063)	0.088 (0.134)	0.143 (0.186)	0.096 (0.183)
shortint.	0.002* (0.001)	0.007*** (0.002)	0.013*** (0.004)	0.013*** (0.004)	0.002** (0.001)	0.008*** (0.002)	0.015*** (0.004)	0.015*** (0.004)
$R^2$ -Adj.	5.0%	5.3%	5.2%	4.9%	4.9%	4.8%	4.0%	3.9%

Notes:

\*\*\*Significant at the 1 percent level.

\*\*Significant at the 5 percent level.

\*Significant at the 10 percent level.

Table 7: Tightness of the crash probability bounds: linear regression tests adding characteristics for a 10% crash

This table reports the results from regressing the indicator function of realized equity returns being less than 0.90 on the option-implied bounds as well as other characteristics for firms belonging to the S&P 500 index. The data are monthly from January 1996 to December 2017. The return horizons are one month, three month, six months, and one year. Values in parentheses are standard errors with two-way clustering following [Petersen \(2009\)](#). Adjusted  $R^2$ s are also reported.

Maturity	Lower bound				Upper bound			
	1	3	6	12	1	3	6	12
intercept	−0.003 (0.051)	0.092 (0.076)	0.063 (0.096)	0.167* (0.100)	−0.023 (0.055)	0.085 (0.080)	0.108 (0.098)	0.180* (0.100)
<b>bounds</b>	0.941*** (0.096)	1.074*** (0.128)	1.381*** (0.136)	1.110*** (0.134)	0.730*** (0.094)	0.672*** (0.092)	0.642*** (0.103)	0.445*** (0.096)
beta	−0.0005 (0.017)	−0.036 (0.028)	−0.065* (0.035)	−0.061* (0.034)	0.020 (0.017)	0.012 (0.026)	0.021 (0.032)	0.027 (0.032)
mom	−0.011 (0.012)	−0.0003 (0.018)	0.012 (0.019)	0.014 (0.019)	−0.008 (0.012)	0.006 (0.018)	0.022 (0.020)	0.022 (0.020)
logsize	0.001 (0.003)	−0.003 (0.004)	−0.0004 (0.005)	−0.006 (0.005)	0.0001 (0.003)	−0.005 (0.004)	−0.006 (0.005)	−0.010* (0.005)
bm	−0.017** (0.007)	−0.039*** (0.010)	−0.064*** (0.011)	−0.066*** (0.011)	−0.015** (0.007)	−0.037*** (0.010)	−0.061*** (0.012)	−0.062*** (0.012)
past_vol	0.064 (0.040)	0.060 (0.054)	−0.010 (0.047)	0.081* (0.047)	0.043 (0.035)	0.047 (0.036)	0.006 (0.047)	0.078 (0.048)
gross_prof	−0.014 (0.010)	−0.028* (0.016)	−0.060*** (0.020)	−0.054** (0.021)	−0.013 (0.010)	−0.024 (0.016)	−0.049** (0.022)	−0.045** (0.022)
debt/asset	−0.012 (0.010)	−0.051*** (0.017)	−0.084*** (0.024)	−0.098*** (0.024)	−0.009 (0.010)	−0.048*** (0.018)	−0.081*** (0.025)	−0.090*** (0.026)
cce/cliab.	−0.003* (0.002)	−0.009*** (0.003)	−0.015*** (0.005)	−0.016*** (0.005)	−0.003 (0.002)	−0.007** (0.003)	−0.012*** (0.005)	−0.013*** (0.005)
turnover	−0.007 (0.106)	−0.051 (0.151)	−0.061 (0.163)	0.007 (0.165)	−0.023 (0.106)	−0.063 (0.153)	−0.080 (0.165)	−0.041 (0.165)
d_turnover	0.032 (0.149)	0.251 (0.204)	0.340 (0.234)	0.150 (0.236)	0.066 (0.153)	0.254 (0.199)	0.315 (0.239)	0.195 (0.236)
shortint.	0.005** (0.002)	0.010*** (0.003)	0.018*** (0.004)	0.018*** (0.004)	0.006*** (0.002)	0.012*** (0.003)	0.020*** (0.004)	0.020*** (0.004)
$R^2$ -Adj.	6.1%	4.8%	4.4%	3.8%	6.1%	4.4%	3.4%	3.0%

Notes:

\*\*\*Significant at the 1 percent level.

\*\*Significant at the 5 percent level.

\*Significant at the 10 percent level.

Table 8: Tightness of the crash probability bounds: linear regression tests adding characteristics for a 5% crash

This table reports the results from regressing the indicator function of realized equity returns being less than 0.95 on the option-implied bounds as well as other characteristics for firms belonging to the S&P 500 index. The data are monthly from January 1996 to December 2017. The return horizons are one month, three month, six months, and one year. Values in parentheses are standard errors with two-way clustering following Petersen (2009). Adjusted  $R^2$ s are also reported.

Maturity	Lower bound				Upper bound			
	1	3	6	12	1	3	6	12
intercept	0.029 (0.073)	0.066 (0.097)	0.051 (0.114)	0.217* (0.117)	-0.007 (0.079)	0.068 (0.103)	0.127 (0.119)	0.261** (0.121)
<b>bounds</b>	0.908*** (0.112)	1.002*** (0.158)	1.259*** (0.155)	0.881*** (0.150)	0.777*** (0.107)	0.662*** (0.121)	0.593*** (0.132)	0.326*** (0.121)
beta	0.001 (0.028)	-0.041 (0.032)	-0.057 (0.037)	-0.041 (0.037)	0.028 (0.027)	0.012 (0.031)	0.028 (0.036)	0.032 (0.035)
mom	-0.004 (0.019)	0.007 (0.022)	0.015 (0.021)	0.018 (0.021)	0.0002 (0.019)	0.014 (0.022)	0.025 (0.022)	0.025 (0.021)
logsize	-0.0005 (0.004)	-0.0003 (0.005)	0.00003 (0.006)	-0.006 (0.006)	-0.001 (0.004)	-0.002 (0.005)	-0.004 (0.006)	-0.008 (0.006)
bm	-0.027*** (0.010)	-0.051*** (0.011)	-0.079*** (0.012)	-0.081*** (0.012)	-0.025** (0.010)	-0.050*** (0.012)	-0.077*** (0.013)	-0.078*** (0.013)
past_vol	0.113** (0.054)	0.110* (0.063)	0.067 (0.051)	0.135*** (0.051)	0.071 (0.046)	0.076* (0.044)	0.053 (0.050)	0.124** (0.051)
gross_prof	-0.026* (0.014)	-0.032 (0.020)	-0.055*** (0.021)	-0.047** (0.022)	-0.025* (0.014)	-0.028 (0.020)	-0.045** (0.022)	-0.039* (0.023)
debt_asset	-0.033** (0.015)	-0.070*** (0.021)	-0.114*** (0.026)	-0.123*** (0.027)	-0.029** (0.015)	-0.066*** (0.021)	-0.108*** (0.027)	-0.114*** (0.028)
cce/cliab.	-0.005* (0.003)	-0.011*** (0.004)	-0.016*** (0.005)	-0.016*** (0.005)	-0.004 (0.003)	-0.009** (0.004)	-0.013** (0.005)	-0.013** (0.005)
turnover	-0.061 (0.147)	-0.060 (0.168)	-0.094 (0.177)	-0.054 (0.178)	-0.087 (0.146)	-0.091 (0.170)	-0.143 (0.179)	-0.104 (0.178)
d_turnover	-0.028 (0.219)	0.205 (0.232)	0.253 (0.258)	0.115 (0.262)	0.033 (0.220)	0.251 (0.224)	0.302 (0.260)	0.179 (0.258)
shortint.	0.007** (0.003)	0.014*** (0.004)	0.019*** (0.004)	0.018*** (0.004)	0.008*** (0.003)	0.015*** (0.004)	0.020*** (0.005)	0.019*** (0.005)
$R^2$ -Adj.	3.8%	2.8%	2.9%	2.4%	3.8%	2.5%	2.2%	1.9%

Notes:

\*\*\*Significant at the 1 percent level.

\*\*Significant at the 5 percent level.

\*Significant at the 10 percent level.

Table 9: Area under the curve (AUC) statistics of out-of-sample forecasting using option-implied bounds and characteristic-based procedures

This table reports AUCs of forecasting whether a stock's net return will be less than  $-20\%$  using the option-implied bounds, as well as statistical procedures. Stocks of firms belonging to the S&P 500 index are considered. The data are monthly from January 1996 to December 2017. The return horizons are one month, three month, six months, and one year. The two statistical procedures under consideration are logistic regression and linear regression, both fine tuned by the LASSO variable selection method. The training sample consists the first half of the data (1996-2006) and the testing sample consists the rest. AUC are all calculated from the testing sample.

Maturity	1	3	6	12
Panel A: $q = 0.80$ , down by 20%				
Lower Bound	0.871	0.771	0.723	0.721
Upper Bound	0.874	0.764	0.703	0.695
Char.Logistic-Lasso	0.802	0.720	0.675	0.676
Char.Linear-Lasso	0.832	0.729	0.680	0.679
Panel B: $q = 0.90$ , down by 10%				
Lower Bound	0.760	0.680	0.657	0.644
Upper Bound	0.760	0.673	0.626	0.605
Char.Logistic-Lasso	0.732	0.656	0.625	0.626
Char.Linear-Lasso	0.733	0.639	0.616	0.614
Panel C: $q = 0.95$ , down by 5%				
Lower Bound	0.645	0.609	0.610	0.593
Upper Bound	0.646	0.604	0.578	0.585
Char.Logistic-Lasso	0.636	0.597	0.585	0.584
Char.Linear-Lasso	0.629	0.587	0.574	0.572

Table 10: Summary statistics of CVIX

This table reports the summary statistics of the annualized CVIX index. Stocks under consideration are for firms belonging to the S&P 500 index. The data are monthly from January 1996 to December 2017. The time horizons are one month, two months, six months and one year. To rule out the impacts of outliers, the time-series average is taken for each firm having more than 60 monthly observations. The summary statistics in Panel A are based on the time-series averages for these qualified firms. The cross-sectional average is taken for each month. The summary statistics in Panel B are based on the cross-sectional averages for each month.

Horizon in month	1	3	6	12
Panel A: Time-series averages				
No. of sample firms	700	699	695	695
Min.(%)	3.80	3.79	3.42	3.24
1st Qu.(%)	8.65	8.14	7.68	7.16
Median(%)	10.49	9.79	9.15	8.52
Mean(%)	10.89	10.19	9.52	8.76
3rd Qu.(%)	12.57	11.80	11.02	10.12
Max.(%)	23.17	21.53	19.22	16.58
Std.dev.(%)	3.32	3.11	2.77	2.37
Panel B: Cross-sectional averages				
No. of sample months	264	264	264	264
Min. (%)	2.38	2.87	3.13	3.39
1st Qu. (%)	5.54	5.68	5.65	5.61
Median (%)	9.11	8.77	8.50	8.12
Mean (%)	10.67	9.98	9.31	8.58
3rd Qu. (%)	13.72	12.71	11.62	10.61
Max. (%)	55.45	42.38	32.67	23.98
Std.dev. (%)	7.12	5.71	4.58	3.64

Table 11: CVIX and the expected returns of stocks

This table reports the results from regressing the realized equity returns on the CVIX index by fitting the simple linear regression model

$$\frac{\tau R_{i,t \rightarrow t+\tau}}{R_f} = \alpha + \beta \text{CVIX}_{i,t}(T) + \epsilon_{i,t+\tau},$$

and by fitting the linear regression model with time fixed-effects

$$\frac{\tau R_{i,t \rightarrow t+\tau}}{R_f} = \alpha_t + \beta \text{CVIX}_{i,t}(T) + \epsilon_{i,t+\tau},$$

where  $T = \tau/12$  and  $\text{CVIX}_{i,t}(T)$  is calculated based on equation (16). The sample firms are ones belonging to the S&P 500 index. The data are monthly from January 1996 to December 2017. The return horizons, denoted by  $\tau$ , are one month, three month, six months, and one year. Results in Panel A are from the simple linear regression. Results in Panel B are ones with time fixed-effects. Values in parentheses are standard errors with two-way clustering (Petersen, 2009). Values in square brackets are standard errors from block bootstrap using 2500 bootstrap samples (Martin and Wagner, 2018). Adjusted  $R^2$ s are also reported.

Horizon in month	1	3	6	12
Panel A: Simple linear regressions				
$\alpha$	0.625 (0.837) [0.903]	0.574 (0.645) [0.866]	0.054 (0.452) [0.736]	0.507 (0.242) [0.372]
$\beta$	0.381 (0.830) [0.896]	0.445 (0.631) [0.847]	0.957 (0.433) [0.707]	0.501 (0.222) [0.341]
$R^2$ -Adj.	0.05%	0.20%	1.11%	1.29%
Panel B: Linear regressions with time fixed effects				
$\beta$	0.924 (0.728) [0.740]	0.902 (0.510) [0.647]	1.044 (0.433) [0.775]	0.543 (0.215) [0.386]
$R^2$ -Adj.	21.47%	23.74%	24.10%	24.24%
Projected $R^2$ -Adj.	0.00%	0.23%	0.80%	0.99%

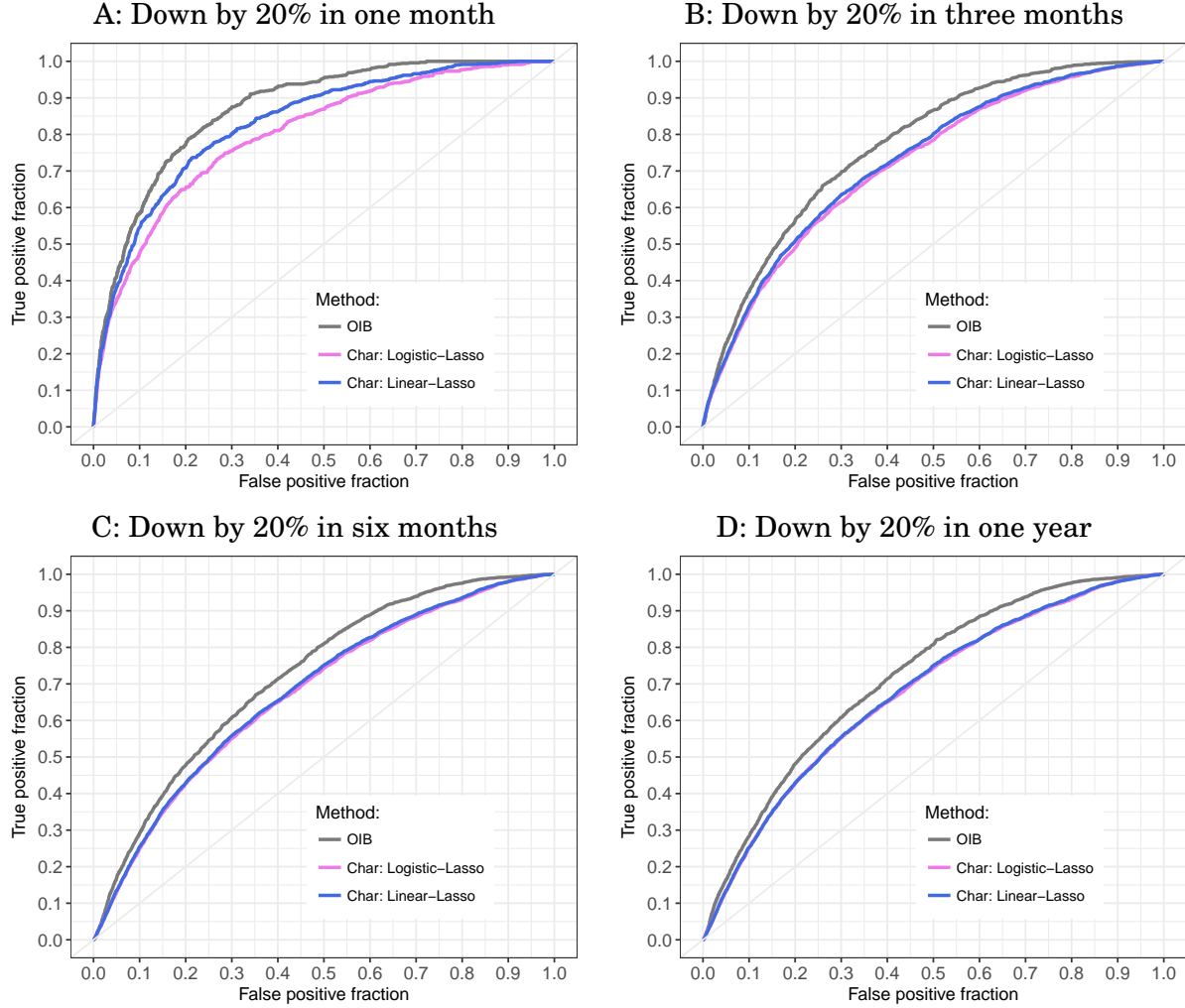


Figure 4: ROC curves of out-of-sample forecasting of crash events: option-implied bounds (OIB) v.s. characteristics-based procedures

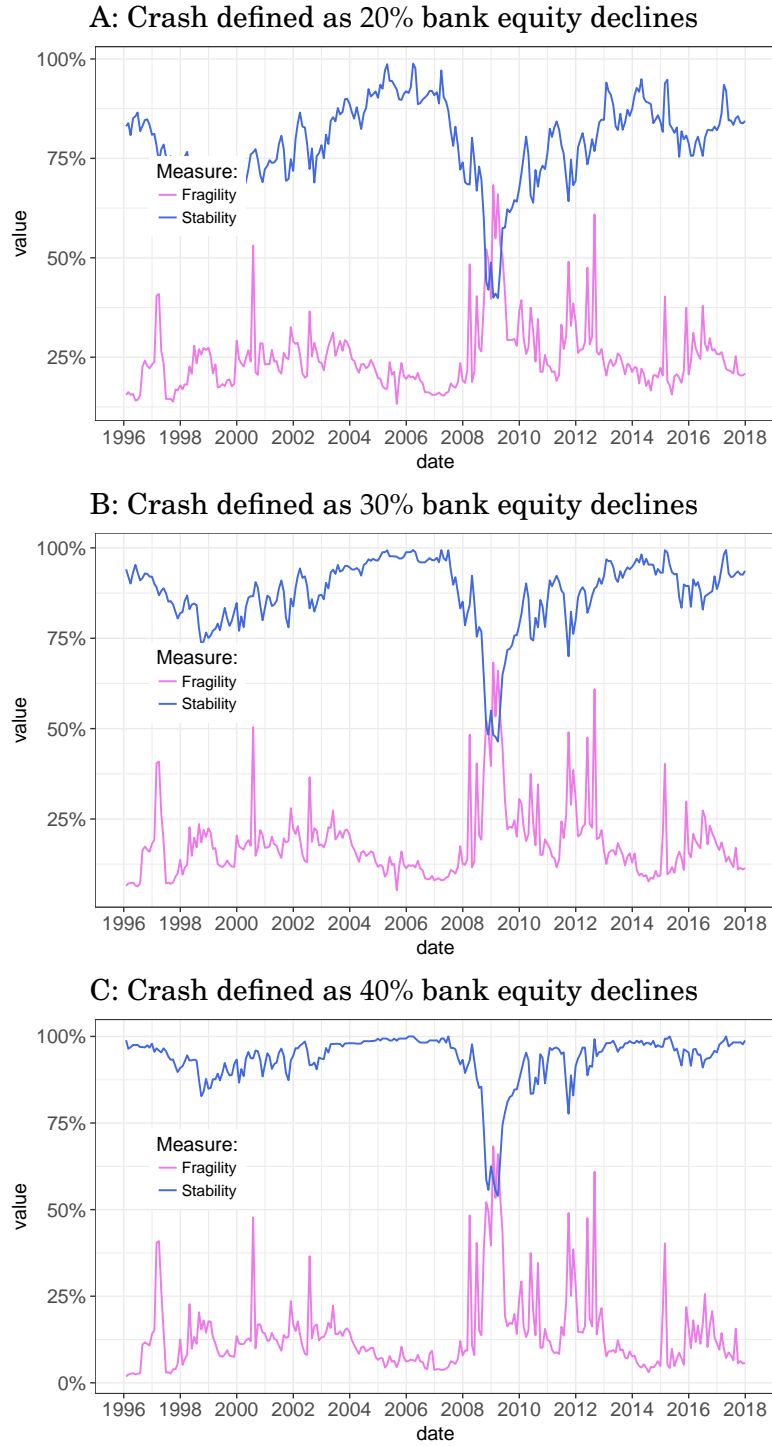
The figures report ROC curves of forecasting whether a stock's net return will be less than  $-20\%$  using the option-implied bounds, as well as statistical procedures. Stocks of firms belonging to the S&P 500 index are considered. The data are monthly from January 1996 to December 2017. The return horizons are one month, three month, six months, and one year. The two statistical procedures under consideration are logistic regression and linear regression, both fine tuned by the LASSO variable selection method. The training sample consists the first half of the data (1996-2006) and the testing sample consists the rest. ROC curves are all based on the testing sample.

Table 12: G-SIBs under consideration

This table lists the twenty-one global systemically important banks (G-SIBs) under study, as subset of all the G-SIBs ever defined by the Financial Stability Board since 2011. The third column reports the period considered as a G-SIB for each bank. The forth column reports the time window within which the option data on each bank's equity are available. To be considered in this analysis, a G-SIB must be either publicly traded in the US or have issued American depositary receipts.

Bank name	Country	FSB G-SIB period	Option sample period
Mizuho FG	Japan	2011-present	2008.10-2017.12
Sumitomo Mitsui FG	Japan	2011-present	2011.06-2017.12
Mitsubishi UFJ FG	Japan	2011-present	1998.02-2017.12
Deutsche Bank	Germany	2011-present	2001.11-2017.12
ING Bank	Netherlands	2011-present	1997.07-2017.12
BBVA	Spain	2012-2015	1998.10-2017.12
Santander	Spain	2011-present	1997.11-2017.12
Credit Suisse	Switzerland	2011-present	2005.03-2017.12
UBS	Switzerland	2011-present	2000.07-2014.12
Barclays	United Kingdom	2011-present	2007.11-2017.12
HSBC	United Kingdom	2011-present	1999.12-2017.12
Lloyds	United Kingdom	2011-2012	2008.10-2017.12
Royal Bank of Canada	Canada	2017-present	2000.10-2017.12
Bank of America	United States	2011-present	1996.01-2017.12
Bank of New York Mellon	United States	2011-present	1996.01-2017.12
Citi	United States	2011-present	1996.01-2017.12
Goldman Sachs	United States	2011-present	1999.08-2017.12
JP Morgan Chase	United States	2011-present	1996.01-2017.12
Morgan Stanley	United States	2011-present	1996.01-2017.12
State Street	United States	2011-present	1996.01-2017.12
Wells Fargo	United States	2011-present	1996.01-2017.12





**Figure 5: Fragility and stability measures of the global banking system**

The figures present the two measures constructed from the crash probability bounds for the global systemically important banks (G-SIBs) introduced in Section 4.2. Both measures are based on one-year crash probability bounds. At the end of each month from 1996-2017, the (cross-sectional) maximum of the lower bounds among the G-SIBs is the fragility measure, and one minus the minimum of the upper bounds is the stability measure. Each panel corresponds to a specific choice of  $q$  in defining a crash event.

# Appendices

## A Proofs

### A.1 Proof of Result 1

*Proof.* When the function  $h$  is increasing, the integrand

$$k(u, v) = \left[ Q_m^{-1}(u) \right]^\gamma h \left( Q_i^{-1}(v) \right)$$

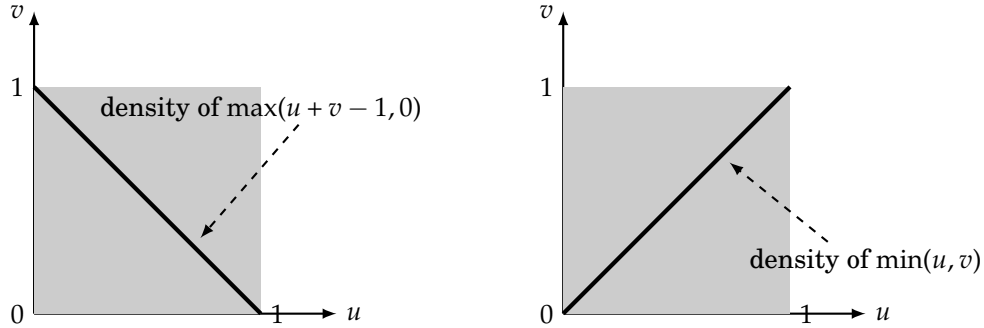
is two-increasing. Based on Corollary 2.2 of Tchen (1980) and the Fréchet-Heoffding (F-H) theorem,

$$\int_{[0,1]^2} \left[ Q_m^{-1}(u) \right]^\gamma h \left( Q_i^{-1}(v) \right) du dv \geq \int_{[0,1]^2} \left[ Q_m^{-1}(u) \right]^\gamma h \left( Q_i^{-1}(v) \right) d(\max(u + v - 1, 0)),$$

and

$$\int_{[0,1]^2} \left[ Q_m^{-1}(u) \right]^\gamma h \left( Q_i^{-1}(v) \right) du dv \leq \int_{[0,1]^2} \left[ Q_m^{-1}(u) \right]^\gamma h \left( Q_i^{-1}(v) \right) d(\min(u, v)).$$

The probability densities of the F-H lower bound,  $\max(u + v - 1, 0)$ , and the F-H upper bound,  $\min(u, v)$ , are uniformly distributed along the two diagonals of the square  $[0, 1]^2$  in  $\mathbb{R}^2$ , illustrated as follows:



Integrating with regard to these two densities and noticing that the denominators both result from a change of variable for  $\mathbb{E}^*[R_m^\gamma] = \int R_m^\gamma dQ_m(R_m)$  will deliver the result.  $\square$

### A.2 Proof of Result 2

*Proof.* With increasing  $h$ , the lower bound is achieved as the copula for the joint risk-neutral distribution of  $(R_m, R_i)$  being  $\max(u + v - 1, 0)$ , that is, the joint risk-neutral CDF of  $(Q_m(R_m), Q_i(R_i))$  is  $\max(u + v - 1, 0)$ . This implies that  $Q_m(R_m) + Q_i(R_i) \equiv 1$ . Similarly, when achieving the lower bound, the joint risk-neutral CDF of  $(Q_m(R_m), Q_i(R_i))$  is  $\min(u, v)$ , which implies that  $Q_m(R_m) = Q_i(R_i)$ .  $\square$

### A.3 Proof of Result 3

*Proof.* Without loss of generality, I focus on the case when  $h$  is increasing. If  $h$  is decreasing, all the arguments below will follow for  $-h$ .

First, when  $\gamma = 0$ , the bounds become

$$\int_0^1 h(Q_i^{-1}(1-u)) \, du \leq \mathbb{E}[h(R_i)] \leq \int_0^1 h(Q_i^{-1}(u)) \, du.$$

A change of variable will lead to  $\int_0^1 h(Q_i^{-1}(1-u)) \, du = \int_0^1 h(Q_i^{-1}(u)) \, du$ , that is, the lower bound equals the upper bound. And clearly, they both equal  $\mathbb{E}^*[h(R_i)]$ .

Second, define  $\psi(x) = h(Q_i^{-1}(1 - Q_m(x)))$ , which is a decreasing function, then the lower bound is  $\mathbb{E}^*[R_m^\gamma \psi(R_m)] / \mathbb{E}^*[R_m^\gamma]$ . Differentiating with regard to  $\gamma \in (0, \infty)$ :

$$\begin{aligned} \frac{d}{d\gamma} \left\{ \frac{\mathbb{E}^*[R_m^\gamma \psi(R_i)]}{\mathbb{E}^*[R_m^\gamma]} \right\} &= \frac{\gamma \mathbb{E}^*[R_m^{\gamma-1} \psi(R_m)] \mathbb{E}^*[R_m^\gamma] - \gamma \mathbb{E}^*[R_m^\gamma \psi(R_m)] \mathbb{E}^*[R_m^{\gamma-1}]}{\{\mathbb{E}^*[R_m^\gamma]\}^2} \\ &= \frac{\gamma}{\{\mathbb{E}^*[R_m^\gamma]\}^2} \iint (x^{\gamma-1} \psi(x) y^\gamma - x^\gamma \psi(x) y^{\gamma-1}) \, dQ_m(x) \, dQ_m(y) \\ &\leq \frac{\gamma}{\{\mathbb{E}^*[R_m^\gamma]\}^2} \left[ \iint_{x \geq y} x^{\gamma-1} y^{\gamma-1} \psi(y) (y-x) \, dQ_m(x) \, dQ_m(y) \right. \\ &\quad \left. + \iint_{x \leq y} x^{\gamma-1} y^{\gamma-1} \psi(x) (y-x) \, dQ_m(x) \, dQ_m(y) \right] \\ &= \frac{\gamma}{\{\mathbb{E}^*[R_m^\gamma]\}^2} \left[ \iint_{x \leq y} x^{\gamma-1} y^{\gamma-1} \psi(x) (x-y) \, dQ_m(x) \, dQ_m(y) \right. \\ &\quad \left. + \iint_{x \leq y} x^{\gamma-1} y^{\gamma-1} \psi(x) (y-x) \, dQ_m(x) \, dQ_m(y) \right] \\ &= 0. \end{aligned}$$

The only inequality is due to that fact that when  $x \geq y$ ,  $\psi(y) \leq \psi(x)$ . Thus the lower bound is decreasing with regard to the risk-aversion parameter  $\gamma$ . Similar technique can be applied when  $\psi(x) = h(Q_i^{-1}(Q_m(x)))$  is an increasing function, which leads to the conclusion that the upper bound is increasing with regard to  $\gamma$ .

Third, noticing that if  $h$  is uniformly bounded and  $\inf_x h(x) = h_{\min}$ , then the lower bound must be such that

$$\frac{\int_0^1 [Q_m^{-1}(u)]^\gamma h(Q_i^{-1}(1-u)) \, du}{\int_0^1 [Q_m^{-1}(u)]^\gamma \, du} \geq h_{\min},$$

for all  $\gamma \geq 0$ . And since the lower bound is decreasing with regard to  $\gamma$ , it will converge to  $h_{\min}$  as  $\gamma \rightarrow \infty$  due to standard monotone convergence arguments. Similarly, the upper bound will converge to  $h_{\max} = \sup_x h(x)$  as  $\gamma \rightarrow \infty$ .  $\square$

## A.4 Proof of Result 4

*Proof.* Under the statement of Result 1, let  $h(R_i) = -I(R_i \leq q)$ , which is an increasing function. Applying Result 1,

$$\begin{aligned}\mathbb{P}[R_i \leq q] &= -\mathbb{E}[h(R_i)] \\ &\geq -\frac{\int_0^1 [Q_m^{-1}(u)]^\gamma h(Q_i^{-1}(u)) \, du}{\int_0^1 [Q_m^{-1}(u)]^\gamma \, du}.\end{aligned}$$

The opposite of the previous upper bound now serves as a lower bound for the crash probability, because  $I(R_i \leq q)$  is decreasing. Plugging in the indicator function form of  $h(R_i)$  and simplifying the integral on the numerator will give rise to

$$\mathbb{P}[R_i \leq q] \geq \frac{\int_0^{Q_i(q)} [Q_m^{-1}(u)]^\gamma \, du}{\int_0^1 [Q_m^{-1}(u)]^\gamma \, du}.$$

This lower bound is achieved when  $Q_i(R_i) = Q_m(R_m)$  according to Result 2, that is, when the stock and market returns are comonotonic under the risk-neutral probability. And similarly,

$$\begin{aligned}\mathbb{P}[R_i \leq q] &= -\mathbb{E}[h(R_i)] \\ &\leq -\frac{\int_0^1 [Q_m^{-1}(u)]^\gamma h(Q_i^{-1}(1-u)) \, du}{\int_0^1 [Q_m^{-1}(u)]^\gamma \, du} \\ &= \frac{\int_0^1 [Q_m^{-1}(u)]^\gamma I(1 - Q_i(q) \leq u \leq 1) \, du}{\int_0^1 [Q_m^{-1}(u)]^\gamma \, du}.\end{aligned}$$

The opposite of the previous lower bound now serves as an upper bound for the crash probability. Again, plugging in the definition of  $h(R_i)$  will give us

$$\mathbb{P}[R_i \leq q] \leq \frac{\int_{1-Q_i(q)}^1 [Q_m^{-1}(u)]^\gamma \, du}{\int_0^1 [Q_m^{-1}(u)]^\gamma \, du},$$

The upper bound above is achieved when  $Q_i(R_i) + Q_m(R_m) = 1$ , again according to Result 2, that is, when stock and market returns are countermonotonic under the risk-neutral probability.  $\square$

## A.5 Proof of Result 5

*Proof.* Consider, again, the stock return contingent payoff  $h(R_i) = -I(R_i \leq q)$ . As the lower bound for  $\mathbb{P}[R_i \leq q]$  is achieved, stock and market returns are comonotonic under the risk-neutral probability. The

risk-neutral beta for stock  $i$ ,

$$\begin{aligned}\beta_i^* &= \frac{\text{cov}^*[R_m, R_i]}{\text{var}^*[R_m]} \\ &= \frac{\mathbb{E}^*[R_m R_i] - R_f^2}{\text{var}^*[R_m]} \\ &= \frac{\int_0^1 Q_m^{-1}(u) Q_i^{-1}(u) du - R_f^2}{\text{var}^*[R_m]},\end{aligned}$$

is maximized since  $\mathbb{E}^*[R_m R_i] \leq \int_0^1 Q_m^{-1}(u) Q_i^{-1}(u) du$  due to Corollary 2.2 of Tchen (1980) and the Fréchet-Heoffding upper bound, fixing the two risk-neutral marginals. Correspondingly,  $\rho_i^* = \beta_i^* \sqrt{\text{var}^*[R_m]/\text{var}^*[R_i]}$  is maximized.

Similarly, as the upper bound for  $\mathbb{P}[R_i \leq q]$  is achieved, stock and market returns are countermonotonic under the risk-neutral probability, and

$$\beta_i^* = \frac{\int_0^1 Q_m^{-1}(u) Q_i^{-1}(1-u) du - R_f^2}{\text{var}^*[R_m]},$$

is minimized since  $\mathbb{E}^*[R_m R_i] \geq \int_0^1 Q_m^{-1}(u) Q_i^{-1}(1-u) du$  due to Corollary 2.2 of Tchen (1980) and the Fréchet-Heoffding lower bound. As a result, the risk-neutral correlation  $\rho_i^*$  is also minimized.

To prove the third part of this result, we can now use, without proof, part 2 of Result 6 (Detailed proof will follow in the next subsection). Under the log-normal example,  $\rho_i^* \leq (e^{\sigma_i \sigma_m} - 1) / \sqrt{(e^{\sigma_i^2} - 1)(e^{\sigma_i} - 1)}$ , which is (strictly) smaller than one if  $\sigma_i \neq \sigma_m$ , that is, the risk-neutral volatilities of the market and stock returns are not equal. And  $\rho_i^* \geq (e^{-\sigma_i \sigma_m} - 1) / \sqrt{(e^{\sigma_i^2} - 1)(e^{\sigma_i} - 1)}$ , which must be (strictly) greater than minus one as  $\max\{\sigma_i, \sigma_m\}$  does not go to zero. This example suffices to proof the statement.  $\square$

## A.6 Proof of Result 6

*Proof.* First,  $\beta_i$  is maximized under comonotonicity, that is,  $Q_i(R_i) = Q_m(R_m)$ . Under the assumption of log-normality,

$$\begin{aligned}\beta_i^* &\leq \frac{\mathbb{E}^*[R_m Q_i^{-1}(Q_m(R_m))] - R_f^2}{\text{var}^*[R_m]} \\ &= \frac{\exp\left(\mu_i - \frac{\sigma_i}{\sigma_m} \mu_m\right) \mathbb{E}^*\left[R_m^{\left(1 + \frac{\sigma_i}{\sigma_m}\right)}\right] - R_f^2}{\mathbb{E}^{*2}[R_m] [\exp(\sigma_m^2) - 1]} \\ &= \frac{\exp\left[\mu_i - \frac{\sigma_i}{\sigma_m} \mu_m + \mu_m \left(1 + \frac{\sigma_i}{\sigma_m}\right) + \frac{1}{2} \sigma_m^2 \left(1 + \frac{\sigma_i}{\sigma_m}\right)^2\right] - R_f^2}{R_f^2 [\exp(\sigma_m^2) - 1]} \\ &= \frac{e^{\sigma_i \sigma_m} - 1}{e^{\sigma_m^2} - 1}.\end{aligned}$$

Similarly,  $\beta_i^*$  is minimized under countermonotonicity, that is,  $Q_i(R_i) + Q_m(R_m) = 1$ . Again, bringing in the assumption of log-normality,

$$\begin{aligned}
\beta_i^* &\geq \frac{\mathbb{E}^* \left[ R_m Q_i^{-1}(1 - Q_m(R_m)) \right] - R_f^2}{\text{var}^*[R_m]} \\
&= \frac{\exp \left( \mu_i + \frac{\sigma_i}{\sigma_m} \mu_m \right) \mathbb{E}^* \left[ R_m^{\left(1 - \frac{\sigma_i}{\sigma_m}\right)} \right] - R_f^2}{\mathbb{E}^{*2}[R_m] [\exp(\sigma_m^2) - 1]} \\
&= \frac{\exp \left[ \mu_i + \frac{\sigma_i}{\sigma_m} \mu_m + \mu_m \left( 1 - \frac{\sigma_i}{\sigma_m} \right) + \frac{1}{2} \sigma_m^2 \left( 1 - \frac{\sigma_i}{\sigma_m} \right)^2 \right] - R_f^2}{R_f^2 [\exp(\sigma_m^2) - 1]} \\
&= \frac{e^{-\sigma_i \sigma_m} - 1}{e^{\sigma_m^2} - 1}.
\end{aligned}$$

Second, the results for  $\rho_i^*$  quickly follows from that fact that  $\rho^* = \beta_i^* \sqrt{(e^{\sigma_m^2} - 1)/(e^{\sigma_i^2} - 1)}$  under the log-normality assumption.

Third, when the physical crash probability is minimized, according to Result 4 and the fact that  $R_m^\gamma$  is also log-normal, the lower bound is

$$\begin{aligned}
\frac{\int_0^{Q_i(q)} \left[ Q_m^{-1}(u) \right]^\gamma du}{\int_0^1 \left[ Q_m^{-1}(u) \right]^\gamma du} &= \frac{\mathbb{E}^*[R_m^\gamma \mid R_m^\gamma \leq \{Q_m^{-1}(Q_i(q))\}^\gamma] \times \mathbb{P}[Q_m(R_m) \leq Q_i(q)]}{\mathbb{E}^*[R_m^\gamma]} \\
&= \Phi \left( \frac{\gamma \log [Q_m^{-1}(Q_i(q))] - \gamma \mu_m - \gamma^2 \sigma_m^2}{\gamma \sigma_m} \right) e^{-\gamma \mu_m - \frac{1}{2} \gamma^2 \sigma_m^2},
\end{aligned}$$

while  $Q_m^{-1}(Q_i(q)) = e^{\frac{\log q - \mu_i}{\sigma_i} \sigma_m + \mu_m}$  due to the log-normality of the two margins. Plugging this expression in and simplify will lead to

$$\frac{\int_0^{Q_i(q)} \left[ Q_m^{-1}(u) \right]^\gamma du}{\int_0^1 \left[ Q_m^{-1}(u) \right]^\gamma du} = \Phi \left( \frac{\log q - \mu_i}{\sigma_i} - \gamma \sigma_m \right).$$

And for the upper bound

$$\begin{aligned}
\frac{\int_{1-Q_i(q)}^1 \left[ Q_m^{-1}(u) \right]^\gamma du}{\int_0^1 \left[ Q_m^{-1}(u) \right]^\gamma du} &= \frac{\mathbb{E}^*[R_m^\gamma \mid R_m^\gamma \geq \{Q_m^{-1}(1 - Q_i(q))\}^\gamma] \times \mathbb{P}[Q_m(R_m) \geq 1 - Q_i(q)]}{\mathbb{E}^*[R_m^\gamma]} \\
&= \Phi \left( \frac{\gamma \mu_m + \gamma^2 \sigma_m^2 - \gamma \log [Q_m^{-1}(1 - Q_i(q))]}{\gamma \sigma_m} \right) e^{-\gamma \mu_m - \frac{1}{2} \gamma^2 \sigma_m^2}.
\end{aligned}$$

Given that  $Q_m^{-1}(1 - Q_i(q)) = e^{\frac{\mu_i - \log q}{\sigma_i} \sigma_m + \mu_m}$ , plugging into the expression above for the upper bound,

$$\frac{\int_{1-Q_i(q)}^1 [Q_m^{-1}(u)]^\gamma du}{\int_0^1 [Q_m^{-1}(u)]^\gamma du} = \Phi\left(\frac{\log q - \mu_i}{\sigma_i} + \gamma \sigma_m\right).$$

Let  $\gamma \rightarrow 0$ , based on the convergence property of the bounds in Result 3, the risk-neutral crash probability  $\mathbb{P}^*[R_i \leq q]$  must be  $\Phi\left(\frac{\log q - \mu_i}{\sigma_i}\right)$ , where  $\mu_i = \log R_f - \frac{1}{2}\sigma_i^2$ . Thus

$$p^* = \Phi\left[\frac{1}{\sigma_i} \log\left(\frac{q}{R_f}\right) + \frac{1}{2}\sigma_i\right].$$

Plugging this equation back to the expressions for the lower and upper bounds leads to the conclusion.  $\square$

## B Details about recovering risk-neutral marginals

### B.1 Shape-constrained refinements and ruling out arbitrage opportunities

This section presents implementation details about recovering the risk-neutral marginal distributions from the option prices. At a specific date, let  $x_i = K_i$ ,  $i = 1, 2, \dots$ , be the available strike prices of a certain option contract (on a specific underlying with a given maturity); let  $y_i = \text{put}(K_i)$  if  $K_i \leq R_f S_0$  (i.e., out-of-the-money put prices), and  $y_i = \text{call}(K_i) + K_i/R_f - S_0$  if  $K_i > R_f S_0$  (i.e., put prices implied by the out-of-the-money call prices under the put-call parity). Treating the  $(x_i, y_i)$  pairs as observables, the following nonparametric shape-constrained model is fitted:

$$\min_{f \in \mathcal{F}} \left\{ \sum_i [y_i - f(x_i)]^2 + \frac{1}{2} \lambda \|f\|_2^2 \right\}$$

where  $\mathcal{F} = \{f \in \mathcal{C}(\mathbb{R}_+) : f > 0, f' > 0, f'' > 0\}$  is the set of continuous functions defined on  $\mathbb{R}_+$  that are both monotonically increasing and convex (to rule out arbitrage opportunities along the moneyness dimension). This nonparametric fitting is implemented via the shape-constrained B-spline basis approach of [Pya and Wood \(2015\)](#). The tuning parameter  $\lambda$  is chosen via standard generalized cross-validation procedures following [Pya and Wood \(2015\)](#).

Based on the nonparametric fitting outcomes, smooth relationship between option prices and strike prices is obtained with refined details. Arbitrage is also ruled out along side the moneyness dimension. Taking derivatives according to (13) generates the risk-neutral marginal distribution.

### B.2 Deep out-of-the-money (DOOM) option prices

Option prices and implied volatilities are not observed for extremely out-of-the-money contracts. For volatility surfaces from OptionMetrics, data are only available for options with (the absolute values of) option deltas greater than 0.2 and smaller than 0.8. And the resulting ratio of  $K/S_0$  is almost always within the

interval (0.5, 1.5), for the time horizons under consideration in the paper.

The nonparametric recovering approach needs information about DOOM option prices to capture the tail behavior of the risk-neutral marginals. To address this issue, I make the following assumption:

**Assumption B.1.** *The volatility surface flattens out as the absolute value of log moneyness becomes very large.*

Based on this assumption, I can approximate the unobservable DOOM implied volatilities with the nearest available ones on the volatility surface<sup>21</sup>. Specifically, let  $K_0 \leq K_1 \leq \dots \leq K_{n-1} \leq K_n$  be the strike prices at which implied volatilities are observed. The for any  $0 < K \leq K_0$ , I assume  $\sigma(K) = \sigma(K_0)$  and for any  $K \geq K_n$ , I assume  $\sigma(K) = \sigma(K_n)$ , where  $\sigma(K)$  represents the implied volatility at strike price  $K$ , given the underlying and maturity at a certain time.

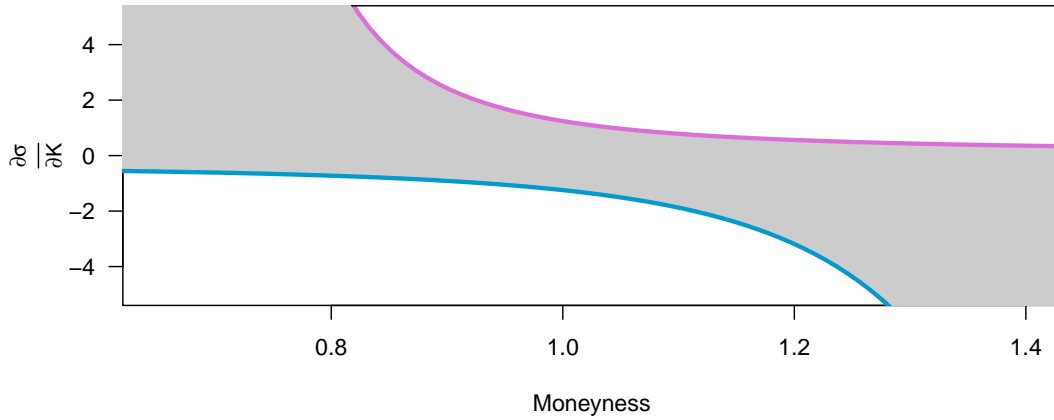


Figure 6: No-arbitrage bounds for the implied volatility

The following proposition provides an asymptotic justification for the assumption above. Figure 6 illustrates the behavior of  $\frac{\partial \sigma_{imp}}{\partial K}$ : as the absolute value of the log-moneyness becomes large, the implied volatility cannot always keep increasing.

**Proposition B.1.** *Let  $x = \log\left(\frac{K}{S_0 R_f}\right)$  be the log-moneyness and of an option maturing in time  $\tau$ , and  $\sigma_{imp}(x)$  be the Black-Scholes implied volatility at strike  $K$ . Define*

$$d_1 = -\frac{x}{\sigma_{imp}(x)\sqrt{\tau}} + \frac{\sigma_{imp}(x)\sqrt{\tau}}{2}, \quad d_2 = -\frac{x}{\sigma_{imp}(x)\sqrt{\tau}} - \frac{\sigma_{imp}(x)\sqrt{\tau}}{2}.$$

Assuming there is no arbitrage,

$$-\frac{1}{K\sqrt{\tau}} \frac{\Phi(-d_1)}{\phi(d_1)} \leq \frac{\partial \sigma_{imp}}{\partial K} \leq \frac{1}{K\sqrt{\tau}} \frac{\Phi(d_2)}{\phi(d_2)},$$

<sup>21</sup>Here, nearest is only defined through distances along the moneyness dimension.



where  $\Phi(\cdot)$  is the standard normal CDF and  $\phi(\cdot)$  is the standard normal density function.

*Proof.* For the European call option price  $\text{call}(K)$ , under no arbitrage,

$$\frac{\partial \text{call}(K)}{\partial K} \leq 0.$$

The Black-Scholes implied volatility  $\sigma_{imp}(x)$  with  $x = \log\left(\frac{K}{S_0 R_f}\right)$  is such that

$$\text{call}(K) = S_0 \Phi(d_1) - \frac{K}{R_f} \Phi(d_2).$$

Taking first-order derivatives on both sides of the equation with regard to  $K$  yields

$$0 \leq \frac{\partial \text{call}(K)}{\partial K} = S_0 \phi(d_1) \left( \frac{\partial d_1}{\partial K} + \frac{\partial d_1}{\partial \sigma_{imp}} \frac{\partial \sigma_{imp}}{\partial K} \right) - \frac{1}{R_f} \Phi(d_2) - \frac{K}{R_f} \phi(d_2) \left( \frac{\partial d_2}{\partial K} + \frac{\partial d_2}{\partial \sigma_{imp}} \frac{\partial \sigma_{imp}}{\partial K} \right).$$

Notice that, by definition,

$$\frac{\partial d_1}{\partial \sigma_{imp}} = -\frac{d_2}{\sigma_{imp}}, \quad \frac{\partial d_2}{\partial \sigma_{imp}} = -\frac{d_1}{\sigma_{imp}}.$$

Plugging these equations back in and simplify with deliver the right hand side of the inequality. The left hand side can be shown similarly. □